Aus der Chirurgischen Klinik,
Campus Charité Mitte und Campus Virchow-Klinikum
der Medizinischen Fakultät Charité – Universitätsmedizin Berlin

DISSERTATION

Proteomic analysis of the native and fibrotic human
liver matrisome for organ engineering

Proteomische Analyse des nativen und fibrotischen humanen
Lebermatrisoms für Organ Engineering

zur Erlangung des akademischen Grades
Medical Doctor - Doctor of Philosophy (MD/PhD)

vorgelegt der Medizinischen Fakultät
Charité – Universitätsmedizin Berlin

von

Assal Daneshgar

aus Berlin

Datum der Promotion: 25. Juni 2023

This thesis is based on the scientific concept, devised and employed techniques, main results, and potential clinical applications introduced in the publications *'The human liver matrisome – Proteomic analysis of native and fibrotic human liver extracellular matrices for organ engineering approaches'* published in *Biomaterials (2020)* and *'Teburu – Open source 3D printable bioreactor for tissue slices as dynamic three-dimensional cell culture models'* published in *Artificial Organs (2019)* and *'Outcomes of Liver Resections after Liver Transplantation at a High-Volume Hepatobiliary Center'* published in *Journal of Clinical Medicine (2020).*

Table of Contents

Abstract

A persistent demand in suitable grafts has underscored the need for the development of bioartificial organs. Despite global effort to innovate novel alternatives, the creation of transplants yet faces fundamental challenges that are related to organ specific functionality and immunogenicity and hinder current approaches from clinical translation. A vital objective to successfully implement bioartificial organs into clinical practice is the creation of complex biomaterials that will mediate regenerative capacities for long-lasting performance of newly developed grafts.

In this thesis, I present in-depth analysis of human derived liver extracellular matrices by utilizing a label-free shotgun proteomic approach. By applying various decellularization and defatting strategies to fabricate organotypic tissues for proteomic measurements, this work aims to provide insights into the native human liver matrisome to determine the overall complexity that needs to be taken into account when creating novel biomaterials to be functionalized in the development of bioartificial organs. Furthermore, by utilizing the devised experimental workflow for the analysis of fibrotic and cirrhotic human liver extracellular matrices, proteomic features were detected that can be potential targets for therapeutic exploitation. In addition to these two intertwining research threads, this thesis introduces a versatile platform to further functionalize the created human liver extracellular matrices by enabling a facile combination of these scaffolds with prevailing technology to successfully translate various bioengineering approaches from concept to therapeutic reality.

The results obtained from human liver matrices support the necessity of including proteomic techniques in interpreting processes underlying tissue homeostasis and regeneration. Proteomic analysis of native tissues provides cues to be utilized in the creation of bioartificial products. This information shall bridge the gap between currently available digital fabrication technology and the clinical usage of functional organ replacements. Furthermore, by analyzing fibrotic and cirrhotic human derived liver scaffolds, specific characteristics were described that demand further investigation to fully understand signaling pathways underlying the emergence of fibrosis and cirrhosis.

Zusammenfassung

Eine anhaltende Nachfrage nach geeigneten Transplantaten hat die Notwendigkeit der Entwicklung bio-artifizieller Organe unterstrichen. Trotz globaler Bemühungen steht die Erzeugung von Transplantaten noch vor grundlegenden Herausforderungen, die mit der organspezifischen Funktionalität und Immunogenität zusammenhängen und aktuelle Ansätze an der klinischen Translation hindern. Ein wichtiges Ziel für die erfolgreiche Einführung bio-artifizieller Organe in die klinische Praxis ist die Entwicklung und Herstellung komplexer Biomaterialien, welche zu Regeneration fähig sind und somit eine langanhaltende biologische Leistung ermöglichen.

Im Rahmen dieser Dissertation führte ich eine eingehende Analyse von extrazellulären Lebermatrizes humanen Ursprungs unter Verwendung eines *label-free shotgun* proteomischen Ansatzes durch. Durch die Anwendung verschiedener Dezellularisierungs- und Entfettungsstrategien zur Herstellung organotypischer Gewebe für proteomische Analysen zielt diese Arbeit darauf ab, Einblicke in das native humane Lebermatrisom zu geben, um die gesamte Komplexität zu bestimmen, die bei der Herstellung neuartiger Biomaterialien zur Entwicklung bio-artifizieller Organe zum Einsatz kommen sollte. Des Weiteren wurde der entworfene experimentelle Arbeitsablauf verwendet, um proteomische Merkmale fibrotischer und zirrhotischer humaner Lebermatrizes zu identifizieren, die potenzielle Ziele für eine therapeutische Nutzung sein können. Zusätzlich zu diesen beiden miteinander verknüpften Forschungsfäden wird in dieser Arbeit eine vielseitig anwendbare Plattform zur umfangreichen Funktionalisierung der extrazellulären Lebermatrizes humanen Ursprungs vorgestellt. Hierdurch soll die Kombination dieser Matrizes mit vorherrschenden Technologien erleichtert werden, um die verschiedenen Ansätze des *Bioengineerings* erfolgreich vom Konzept zur therapeutischen Realität umzusetzen.

Die in dieser Arbeit präsentierten Ergebnisse aus humanen Lebermatrizes unterstreichen die Relevanz proteomischer Techniken bei der Interpretation der Prozesse, die der Gewebehomöostase und -regeneration zugrunde liegen. Die Untersuchung der proteomischen Landschaft natürlicher Gewebe liefert Kenntnisse, die in der Erzeugung bio-artifizieller Produkte verwendet werden können. Diese Informationen sollen die Lücke zwischen verfügbaren digitalen Fertigungstechnologien und dem klinischen Einsatz funktioneller Organersatzprodukte schließen. Darüber hinaus wurden durch die Analyse von fibrotischen und zirrhotischen humanen Lebermatrizes spezifische Eigenschaften beschrieben, die weitere Untersuchungen erfordern, um die der Entstehung von Fibrose und Zirrhose zugrunde liegenden Signalwege vollständig zu verstehen.

1. Introduction

1.1. The Human Matrisome

The human matrisome is an intricate network of a large variety of proteins that collectively form a responsive microenvironment of fundamental importance for surrounding cells [1-3]. By hosting an extensive repertoire of bioactive features, the human matrisome mediates various biological processes for tissue homeostasis and survival [2-4]. Thus, the matrisome represents a novel concept to expound the diverse characteristics of the extracellular space. In the scope of organ engineering, tremendous efforts have been made to shed light on the human proteome in health and disease. In-depth analysis of the various matrisome constituents poses a crucial step in the development of non-immunogenic matrices capable of encapsulating cells and mediating long-lasting performance of bioengineered grafts. Furthermore, such analysis will also contribute to our knowledge of processes that are responsible for organ failure or reasons leading to the necessity of performing retransplantation or resection after transplantation [5]. Moreover, as changes to the highly organized foundation of the human matrisome are expected to trigger the emergence of many diseases, including liver fibrosis and cirrhosis, in-depth analysis of human matrices will contribute immensely to our understanding of the complex processes underlying pathological conditions and will provide promising opportunities to identify characteristic signatures for therapeutic exploitation [6-8]. Despite this vital role of human matrices at the intersection of biomaterial science and regenerative medicine, the human liver matrisome has been insufficiently described. To address this issue, label-free shotgun proteomics were utilized to acquire extensive data from human derived healthy, fibrotic and cirrhotic liver extracellular matrices (ECM) that can further be functionalized in a variety of bioengineering approaches [9].

1.2. Decellularization and Biomaterial Science

Decellularization is an exceedingly relevant method to create ECM scaffolds of natural origin, which inherit many characteristics of their human analogues [1]. Existing approaches utilizing these matrices in the production of functional biomaterials range from the creation of injectable acellular ECM-based hydrogels [1], to complex reseedable scaffolds [10,11], to supplemented 3D-printable bioinks for the fabrication of tissues and whole organs [12-14]. Within this context, organ engineering strives to interface biomaterial science with cutting-edge technology for the fabrication of biological and architecturally native matrices to collectively create non-immunogenic artificial organ replacements as well as novel platforms for the development of

advanced therapeutic approaches. Despite the wide application of decellularized ECM for bioengineering purposes, the impact of various decellularization-based strategies on the human matrisome has not yet been sufficiently documented. In response to this issue, shotgun proteomics were employed to study healthy human derived liver ECM scaffolds from four patients that had undergone liver resection for medical indications not related to this study [9]. For this purpose, various fabrication protocols were devised that arise from combining decellularization- and defatting-based strategies to render not only the disposal of immunogenic content but also macroscopic and microscopic lipids to ultimately create naturally sourced biological matrices [9].

1.3. Proteomics to Explore the Human Matrisome

Proteomic technologies have vastly impacted science and medicine by providing the opportunity to precisely capture the myriad of proteins constituting biological samples [15,16]. Thus, proteomic analysis has widely been utilized to describe the human proteome [17]. Generally, "top-down" and "bottom-up" proteomic techniques present two dominant approaches to obtain proteomic data. While top-down approaches correspond to the measurement of intact proteins, bottom-up approaches correspond to the mass spectrometry-based measurement of peptides resulting from the digestion of proteins [18]. The term "shotgun proteomics" further describes the detection of peptides obtained from digesting complex samples [19,20]. Within this scope, shotgun proteomics emerge as the method of choice, due to the more robust *in silico* exploration of proteome constituents [21]. Nevertheless, diverse modifications and heavy cross-linkage of proteins related to the matrisome have posed important hindrances to obtain profound data on the human matrisome [22]. Despite the exponential growth of available solubilization and digestion techniques that focus the analysis on a predetermined fraction of proteins, a sample preparation technique was needed that universally captures the intricacy of ECM proteins. Furthermore, as studies regarding human transplant outcome imply, there is a substantial need to understand factors that may endanger graft performance and may even lead to retransplantation or liver resection after transplantation. Among conceivable factors, immunogenicity of grafts is of especial significance. In this context, proteomic measurements need to represent the overall constituents that should be considered in the field of bioengineering and organ transplantation. In this context, the filter-aided sample preparation method has been documented as a desirable technique to obtain a profound coverage of constituents in diverse biological samples [23] and has especially been reported as a powerful technique for the investigation of tissue samples processed by decellularization [11]. The advantage of this method vastly lies in the removal of sodium dodecyl sulfate that despite widely being utilized for tissues decellularization

may interfere and negatively impact proteomic measurements [11,23]. Thus, this method was utilized to universally prepare the wide pallet of protein within the ECM protein extracts and ultimately generating robust proteomic data for further analysis.

1.4. Approaches in Organ Engineering

Over the long trajectory of creating bioartificial organ replacements, great efforts have been made to disintegrate various components of native organs and subsequently unifying material, form and function to create newly engineered implantable off-the-shelf grafts. Fundamental advances unlocking such paths for the creation of functional organ replacements include the advancement of digital fabrication platforms that allow a precise placement of cells and matrices into defined shapes [12,24,25], and the distribution of 3D printable decellularized ECM-supplemented bioinks distinctly impacting cellular response [13]. Nevertheless, to successfully interface prevailing microfabrication techniques with cellular functionality for the creation of bioartificial organ replacements, extensive information regarding the complex proteomic landscape of the human matrisome is required to develop non-immunogenic biomaterials based on the natural human counterpart. To address this issue, this thesis presents a shotgun proteomic approach to determine proteins related to the human liver matrisome by utilizing various ECM scaffold fabrication protocols.

Beyond the confines of utilizing decellularized ECM in top-down and bottom-up biofabrication techniques, patient-derived ECM scaffolds hold great potential as personalized platforms for the development and evaluation of novel therapeutic approaches [26]. Furthermore, such platforms of natural origin can be of extraordinary value to investigate cell-cell and cell-matrix interactions [27,28], especially when combined with currently available technology, such as optogenetic approaches to directly target and influence cells with a high spatio-temporal resolution [29-31]. Accordingly, standardized bioreactor systems, enabling a facile combination of patient-derived ECM scaffolds with novel approaches for targeted tissue repair, need to be introduced to fully harness the wide applications of such platforms. For this reason, the easy-to-handle, multi-purpose, and cost-effective 3D-printable bioreactor *Teburu* was created to provide a controlled and optimized environment for the dynamic cultivation of tissue slices [32]. As an open-source customizable engineering platform, *Teburu* shall expand the ways in which extracellular matrices can be utilized by bioengineers to overcome shortcomings in scalability, controllability and reproducibility of material-driven cell signaling on an individual and collective level.

1.5. Hypothesis and Aim of this Study

Prevailing technology and current shortcomings in the development of functional organ replacements lead to the hypothesis that a deeper understanding of human liver matrisome compositions will solve prevalent problems related to immunogenicity and long-term functionality of newly engineered biomaterials. Based on this hypothesis, I aimed to define the human liver matrisome by employing label-free shotgun proteomics. I hereby aimed to specify features for long-lasting performance of bioengineered organ replacements. Under the premise that changes to the highly organized human liver matrisome underlie the emergence of diseases, I further employed the devised proteomic workflow to investigate fibrotic and cirrhotic human liver extracellular matrices to find possible targets for therapeutic utilization. In addition, I aimed to provide a standardized and multi-purpose platform to further functionalize the created ECM scaffolds for various bioengineering approaches.

2. Materials and Methods

2.1. Materials

Materials that were used in this study are listed below by category and in the chronological order in which they were employed.

Equipment	Company	Application
Unimax 2010	Heidolph Instruments GmbH & CO. KG, 91126 Schwabach, Germany	Decellularization and Defatting
Milli-Q®	Merck Chemicals GmbH, Darmstadt 64293, Germany	Water Purification
Mixer Mill MM400	Retsch GmbH, 42781 Haan, Germany	Sample Preparation
NanoDropTM 2000/2000c	Thermo Fischer Scientific, Waltham, MA 02451, USA	DNA Quantification
TECAN infinite® M1000 Pro	Tecan Group Ltd., 8708 Maennedorf, Switzerland	TAG Quantification
FLUOstar OPTIMA	BMG LABTECH GmbH, 77799 Ortenberg, Germany	Protein Quantification
Form 2	Formlabs GmbH, 12459 Berlin, Germany	Digital Fabrication
DASGIP MX 4/4	Eppendorf Vertrieb Deutschland GmbH, 50389 Wesseling-Berzdorf, Germany	Oxygenation
Zeiss Axio Observer Z1	Carl Zeiss Microscopy GmbH, 07745 Jena, Germany	Microscopy
Dionex UltiMate 3000 NanoHPLC	Thermo Fisher Scientific, Waltham, MA 02451, USA	Liquid Chromatography Tandem Mass Spectrometry
Impact II	Bruker Dalton GmbH, 28359 Bremen, Germany	Liquid Chromatography Tandem Mass Spectrometry
Bio-Rad ChemiDoc XRS Quantity One 4.6.9	Bio-Rad Laboratories GmbH, 85622 Feldkirchen, Germany	Western Blot

Table 1: List of equipment used in this study.

Software	Company	Application
3DS Max (Educational Version 2018)	Autodesk GmbH, 18379 Munique, Germany	Digital Fabrication
Preform	Formlabs GmbH, 12459 Berlin, Germany	Digital Fabrication
Star-CCM+	CD-Adapco, Melville, NY, USA	Fluid Dynamics
Zen Pro Software	Carl Zeiss Microscopy GmbH, 07745 Jena, Germany	Microscopy
Instant-Expertise	Brucker Daltonic GmbH, 28359 Bremen, Germany	Proteomic Analysis
ProteinScape (Version 3.0)	Brucker Daltonic GmbH, 28359 Bremen, Germany	Proteomic Analysis
Mascot Server (Version 2.4.1)	Matrix Science Inc., Boston, MA 02110, USA	Proteomic Analysis
Quantity One 4.6.9	Bio-Rad Laboratories GmbH, 85622 Feldkirchen, Germany	Western Blot Analysis
Microsoft Excel Office 365 (Version 15.24)	Microsoft, Redmont, WA 98052, USA	Statistical Analysis
GraphPad Prism (Version 8.1.1)	GraphPad Software, La Jolla, CA 92108, USA	Statistical Analysis

Table 2: List of software used in this study.

Chemicals and Reagents	Company	Application
Sodium Dodecyl Sulfat (SDS)	Carl Roth GmbH, 76185 Karlsruhe, Germany	Decellularization
Triton-X-100	Sigma-Aldrich, St. Louis, MO 63178, USA	Decellularization
Ethanol	Carl Roth GmbH, 76185 Karlsruhe, Germany	Defatting
Propan-2-ol	Carl Roth GmbH, 76185 Karlsruhe, Germany	Defatting
Propan-2-one	Carl Roth GmbH, 76185 Karlsruhe, Germany	Defatting
Nonidet P40	AppliChem GmbH, 64291 Darmstadt, Germany	TAG Quantification
Glycerol Standard Solution	Sigma-Aldrich, St. Louis, MO 63178, USA	TAG Quantification
Free Glycerol Reagent	Sigma-Aldrich, St. Louis, MO 63178, USA	TAG Quantification
Triglyceride Reagent	Sigma-Aldrich, St. Louis, MO 63178, USA	TAG Quantification
2 mM L-Glutamine	Biochrom GmbH, 12247 Berlin, Germany	Cell Culture
Normal Goat Serum	Dako, Agilent Technologies Company, CA 95051, USA	Histology
Mayer's Hematoxylin	Morphisto GmbH, 60314 Frankfurt, Germany	Histology
Eosin Y Solution	Morphisto GmbH, 60314 Frankfurt, Germany	Histology
Oil-Red-O Powder	Sigma-Aldrich, St. Louis, Mo 63178, USA	Histology
Gill's Hematoxylin	Morphisto GmbH, 60314 Frankfurt, Germany	Histology
Propylene-Glycol	Carl Roth GmbH, 76185 Karlsruhe, Germany	Histology
4',6-Diamidino-2-Phenylindole (DAPI)	Sigma-Aldrich, St. Louis, MO 63178, USA	Histology
Pierce™ BCA Protein Reagent A	Thermo Fischer Scientific, Waltham, MA 02451, USA	Protein Quantification
Pierce™ BCA Protein Reagent B	Thermo Fischer Scientific, Waltham, MA 02451, USA	Protein Quantification
Pierce™ Analytical Protein Sandard	Thermo Fischer Scientific, Waltham, MA 02451, USA	Protein Quantification
Tris Base	Sigma-Aldrich, St. Louis, Mo 63178, USA	Proteomic Sample Preparation
Ammonium Bicarbonate (ABC)	Sigma-Aldrich, St. Louis, Mo 63178, USA	Proteomic Sample Preparation
PhosSTOP	Roche GmbH, 68305 Mannheim, Germany	Proteomic Sample Preparation
cOmplete	Roche GmbH, 68305 Mannheim, Germany	Proteomic Sample Preparation
Chaps	Sigma-Aldrich, St. Louis, MO 63178, USA	Proteomic Sample Preparation
Urea	Sigma-Aldrich, St. Louis, MO 63178, USA	Proteomic Sample Preparation
Trypsin	Promega Corporation, Fitchburg, WI 53711, USA	Proteomic Sample Preparation
Trifluoroacetic Acid (TFA)	Merck Chemicals GmbH, Darmstadt 64293, Germany	Proteomic Sample Preparation
Acetonitrile (ACN)	Carl Roth GmbH, 76185 Karlsruhe, Germany	Liquid Chromatography Tandem Mass Spectrometry
Dithiothreitol (DTT)	Sigma-Aldrich, St. Louis, MO 63178, USA	Western Blot
Tris-HCl	Sigma-Aldrich, St. Louis, Mo 63178, USA	Western Blot
Glycin	Merck Chemicals GmbH, Darmstadt 64293, Germany	Western Blot
Pierce™ Reducing Sample Buffer	Thermo Fischer Scientific, Waltham, MA 02451, USA	Western Blot
HiMark™ Pre-stained Protein Standard	Thermo Fischer Scientific, Waltham, MA 02451, USA	Western Blot
Bovine Serum Albumin	Carl Roth GmbH, 76185 Karlsruhe, Germany	Western Blot
Skimmed Milk	Carl Roth GmbH, 76185 Karlsruhe, Germany	Western Blot
Tween 20	AppliChem GmbH, 64291 Darmstadt, Germany	Western Blot
Methanol	Carl Roth GmbH, 76185 Karlsruhe, Germany	Western Blot
Pierce™ ECL Western	Thermo Fischer Scientic, Walham, MA 02451, USA	Western Blot

Table 3: List of chemicals and reagents used in this study.

Kits and Compounds	Company	Application
DNeasy® Blood and Tissue	QIAGEN GmbH, 40724 Hilden, Germany	DNA Quantification
LSAB System-HRP Kit	Dako, Agilent Technologies Company, CA 95051, USA	Immunohistochemistry
Liquid DAB+ Substrate Chromogen System	Dako, Agilent Technologies Company, CA 95051, USA	Immunohistochemistry
Tissue-Tek OCT Cryo-Embedding Compound	Sakura Finetek Germany GmbH, 79219 Staufen, Germany	Histology and Immunohistochemistry
Dako Fluorescence Mounting Medium	Dako, Agilent Technologies Company, CA 95051, USA	Immunohistochemistry
Penicillin	Biochrom GmbH, 12247 Berlin, Germany	Cell Culture
Streptomycin	Biochrom GmbH, 12247 Berlin, Germany	Cell Culture

Table 4: List of kits and compounds used in this study.

Antibodies	Company	Application
Mouse Monoclonal Anti-Collagen I (ab 6308)	Abcam, Cambridge CB4 0FL, UK	Immunohistochemistry
Rabbit Polyclonal Anti-Collagen IV (ab6586)	Abcam, Cambridge CB4 0FL, UK	Immunohistochemistry
Rabbit Polyclonal Anti-Fibronectin (ab2413)	Abcam, Cambridge CB4 0FL, UK	Immunohistochemistry
Rabbit Polyclonal Anti-Laminin (ab11575)	Abcam, Cambridge CB4 0FL, UK	Immunohistochemistry
Rabbit Monoclonal Anti-CD90 (ab92574)	Abcam, Cambridge CB4 0FL, UK	Immunohistochemistry
Proliferating-Cell-Nuclear-Antigen (M0879)	Dako, Agilent Technologies Company, CA 95051, USA	Immunohistochemistry
Goat Anti-Rabbit IgG H&L – Alexa Fluor® 647 (ab150083)	Abcam, Cambridge CB4 0FL, UK	Immunohistochemistry
Goat Anti-Rabbit IgG H&L – Cy 3® (ab6939)	Abcam, Cambridge CB4 0FL, UK	Immunohistochemistry
Goat Anti-Rabbit IgG H&L – Alexa 488® (ab150077)	Abcam, Cambridge CB4 0FL, UK	Immunohistochemistry
Rabbit Polyclonal Anti-Collagen 6A1 (ab151422)	Abcam, Cambridge CB4 0FL, UK	Western Blot
Rabbit Polyclonal Anti-Transglutaminase 2 (ab421)	Abcam, Cambridge CB4 0FL, UK	Western Blot
Mouse Monoclonal Anti-ß-Actin	Sigma-Aldrich, St. Louis, MO 63178, USA	Western Blot
Goat Anti-Rabbit IgG H&L (HRP) (ab205718)	Abcam, Cambridge CB4 0FL, UK	Western Blot
Goat Anti-Mouse IgG H&L (HRP)	Dianova GmbH, 20354 Hamburg, Germany	Western Blot

Table 5: List of antibodies used in this study.

2.2. Production of Human Liver Extracellular Matrix Scaffolds

2.2.1. Acquisition of Samples from Human Livers

Samples from human livers were collected anonymized after obtaining ethical approval in accordance with institutional guidelines (ethics number EA1/289/16). All samples were obtained after informed consent from patients that had undergone liver resection for clinical indications not related to this study. To subject collected specimen to histopathological evaluation, all tissues were collected as duplicates at Charité – Universitätsmedizin Berlin. Specimens were stored at -80 ℃ as 10 x 10 x 10 mm tissue cubes or as fixed samples for histopathological evaluation prior to processing.

2.2.2. Creation of Human Liver Slices

To create human liver slices of 500 µm thickness, collected tissues were frozen sectioned and washed by shaking using 10 ml chilled phosphate buffered saline (PBS: 137 mM sodium chloride, 10 mM disodium hydrogen phosphate, 2.7 mM potassium chloride, 1.8 mM potassium dihydrogen phosphate, pH 7.4) prior to further processing.

2.2.3. Fabrication of Human Liver Extracellular Matrix Scaffolds by Decellularization and Defatting

Tissue scaffolds of natural origin were produced by applying four decellularization and four defatting strategies that were combined to a total number of 16 fabrication protocols [9]. To source acellular matrices from human liver samples, the fabrication process was performed by placing thawed liver slices in sterile 50 ml *Falcon*® conical tubes (Thermo Fischer Scientific, Waltham, MA 02451, USA) containing 10 ml of a detergent. The removal of cellular material and fat was achieved by combining detergents and defatting solvents with continuous shaking at 300 rpm. Decellularization should be performed at room temperature to prevent precipitation of detergents. All fabrication protocols perform decellularization by utilizing SDS or SDS/Triton-X-100 in different concentrations for a total decellularization duration of 24 hours [9]. Although decellularization detergents are widely accepted to not only remove cellular material but also lipids, some human derived liver scaffolds were observed to still contain fat droplets. To obtain matrices free of cellular material and micro- and macroscopic lipids all decellularization protocols were combined with defatting strategies including propan-2-one, propan-2-ol and ethanol [9]. Afterwards all tissue scaffolds were washed for additional 24 h with PBS to remove possible residues of detergents and defatting solvents.

2.2.4. Quantification Assays

To determine the success of the fabrication process genomic deoxyribonucleic acid (DNA) and triacylglyceride (TAG) were quantified.

The success of decellularization was assessed by purifying and quantifying genomic DNA using the commercially available *DNeasy® Blood and Tissue Kit* according to specifications provided by the manufacturer. This protocol includes the disruption of liver tissue and subsequently processing the lysate with different buffers provided with the kit. The kit was used to generate extracts from human liver ECM and non-processed human livers. To measure DNA content in the isolated extracts, a *NanoDrop^{TM} 2000/2000c* spectrometer was used.

The success of defatting was determined by quantifying TAG. Defatted and non-defatted human liver scaffolds were disrupted in 100 µl of 5% Nonidet P40 utilizing a mixer mill [9]. After treating samples in a heating and cooling cycle, the triacylglyceride working reagent – consisting of four parts of the free glycerol reagent and one parts of the triacylglyceride reagent – was added to the resulting supernatant according to specifications provided by the manufacturer. Finally, the TAG content was measured utilizing the multimode microplate reader *TECAN infinite® M1000 Pro*.

2.3. Human Liver Extracellular Matrix Scaffolds as Bioengineering Platforms

2.3.1. Design and Fabrication of the 3D Printable Bioreactor *Teburu*

To create optimal culture condition for the recellularization and dynamic cultivation of tissue slices, the 3D printable bioreactor *Teburu* [32] was designed. The system consists of three main elements: a top and a bottom which together create the perfusion chamber and the fixation table that tightly positions the tissue scaffold inside the recellularization chamber [32]. To create a bioreactor capable of maintaining optimal culture conditions, while operating with only a small volume of culture medium for sustainable cultivation, the reseeding chamber was designed to comprise the perfusing compartment and oxygenating compartment of the bioreactor in the same chamber [32]. To achieve versatile applications of *Teburu* such as its combination with optogenetics, the surface on which the three-dimensional tissue cultures are cultivated directly is fabricated at its thinnest [32]. This way, optogenetic devices can be positioned below the cultivation chamber.

The computational design was generated by utilizing 3DS Max. For digital fabrication of the designed bioreactor *Preform*, the *Formlabs Form 2* stereolithography 3D printer, and the *Dental LT Clear* resin were used. This resin provided by Formlabs allows reusability of the system due to its biocompatible and sterilizable characteristics.

2.3.2. Fluid Dynamic Analysis

The provision of laminar flow poses an important prerequisite for the optimal cultivation of cells and tissues [33]. Hence, the cultivation chamber is designed comprising an elliptical cultivation area to contribute to the maintenance of laminar flow for optimal cultivation of cells [32]. The gas and medium flow were first attained on empirical evidence. To further test these characteristics, fluid dynamics were evaluated by assessing flow behavior in praxis and by computational fluid dynamics (CFD).

Turbulence behavior of the fluid within the cultivation chamber was estimated by calculating the Reynolds number. Accordingly, flow behavior inside the cultivation chamber was predicted by multiplying density and velocity of the flow and the boundary of the flow which corresponds to the diameter of the fixation table bars divided by the dynamic water viscosity. The resulting Reynolds number suggests laminar flow conditions [32]. To further confirm these results computational simulation was performed. For this purpose, the program *Star-CCM+* was utilized to calculate the velocity, pressure and shear stress distribution. Turbulence simulation was performed by employing the k-ω shear stress transport turbulence model to study changes in wall shear stress and pressure considering changes to the overall number of cells [32]. Consequently, the CFD analysis presented laminar flow conditions at a quite low shear stress of 1.2×10^{-4} Pa on the tissue [32].

2.3.3. Static Cell Cultivation

For the recellularization experiment, mesenchymal stroma cells derived from the human umbilical cord (hMSC) were purchased from LGS Standards GmbH and cultivated in traditional culture flasks. The hMSC were grown under sterile conditions with 20 ml of low endotoxin Dulbecco's MEM Medium which was supplemented with 2 mM L-Glutamine, 100 U/ml Penicillin/ Streptomycin, and 10% fetal calf serum. Cultivated hMSC were trypsinized for manual counting after four passages. The number of grown cells was determined using a Neubauer haemocytometer prior to being deployed for recellularization experiments.

2.3.4. Recellularization of Human Liver Extracellular Matrix Scaffolds and Dynamic Cultivation using *Teburu*

Teburu was employed to recellularize human liver ECM with hMSC. For the recellularization experiment, *Teburu* was filled with 15 ml culture medium and hMSC were applied under sterile conditions to the fixed scaffold using a pipette. After closing the system by attaching the top and bottom using a sealing ring and four screws and nuts, *Teburu* was placed in an incubator

at 37 ºC and the oxygenation inlet was connected to an oxygenator. The reseeded scaffold was left for 18 h of static cultivation to ensure a well attachment of cells. After this period the system would start dynamic cultivation with an initial flow rate of 0.1 ml/min. This value was slowly increased to a final flow rate of 0.8 ml/min. For most optimal growth, regular changes of the culture medium should be carried out for the total dynamic cultivation period of seven days. To assess *Teburu's* capability in maintaining optimal culture conditions, oxygenation parameters, pH, electrolytes, glucose, and lactate were obtained using the *ABL800 FLEX* blood gas analyzer for the overall dynamic recellularization time of 7 days during an experiment.

2.3.5. Histology and Immunohistochemistry

Processed and non-processed human liver samples were prepared for frozen sectioning by embedding tissues in *Tissue-Tek* optimal cutting temperature compound (OTC). Sections of 5 µm thickness were processed at -20 ºC and prepared on *SuperFrost Plus*^{TM} adhesion slides. After fixing tissue sections with chilled acetone, the result of decellularization and defatting was assessed by performing Hematoxylin and Eosin (H&E) staining and Oil-Red-O (ORO) staining. To perform H&E staining, horizontally prepared specimens were immersed in Mayer's Hematoxylin solution for 10 min after rehydration and subsequently rinsed for 5 min with lukewarm water. After immersing sections for 1 min in Eosin Y solution, samples were prepared for mounting and visualization. Similarly, ORO staining was performed by immersing sections in 100% propylene-glycol for 10 min after rehydration. Afterwards, sections were incubated for 10 min in ORO working solution followed by elution using a decreasing gradient of propylene glycol. After final immersion in Gill's Hematoxylin solution, specimens were washed and processed for mounting.

Immunohistochemistry was performed for either horizontally prepared ECM sections or vertically prepared recellularized human liver scaffold sections. Created human liver ECM scaffolds were evaluated by immunohistochemical staining of laminin, fibronectin, collagen IV, and collagen I, whereas recellularized human derived liver scaffolds were evaluated by CD90 and Proliferating-Cell-Nuclear-Antigen (PCNA) staining. For this purpose, rehydrated frozen sectioned specimens were blocked using 3% normal goat serum for a total duration of 1 hour. Collagen I was visualized by incubating specimens for 1 hour at 37 ºC with the primary antibody diluted in blocking solution. After washing specimens twice, specimens were subjected to the secondary antibody for another 2 hours. Similarly, laminin, fibronectin, and collagen IV were visualized by applying the antibodies successively. Recellularized human liver specimens were incubated for 1 hour at 37 ºC with the anti-CD90 primary antibody or PCNA. After washing specimen twice, the fluorescent dye-conjugated secondary antibody was applied to samples

treated with anti-CD90 and the labelled streptavidin-biotin method was applied to samples treated with PCNA. All immunohistochemically dyed samples were counterstained with DAPI or Mayer's hematoxylin. Specificity for each staining was confirmed by a negative control. Non-processed human liver samples were stained for better representation. After final mounting, specimens were visualized utilizing the *Zeiss Axio Observer Z1* brightfield and inverted phase contrast fluorescence microscope. The *Zen pro* software was used to acquire all images.

2.4. Proteomic Analysis of Human Liver Extracellular Matrix Scaffolds

2.4.1. Sample Preparation for Label-Free Shotgun Proteomic Analysis

Human liver scaffolds were prepared for proteomic analysis by using the filter-aided sample preparation method [23]. A bead mixer mill was used to thoroughly disrupt ECM samples. The mixing beads were cleansed in-between samples using 100% ethanol. To solubilize proteins, samples were mixed with a buffer comprising 112 mM 3-[(3-cholamidopropyl) dimethylammonio]-1-propanesulfonate (CHAPS), Tris base, and the phosphatase and protease inhibitor cocktail for the maintenance of sample quality [9]. Subsequently, 200 µl 8 M urea diluted in Tris buffer was added to the samples followed by sonication on ice. *Amicon Ultra* 0.5 ml centrifugal filter unites with a 10 kDa nominal molecular weight limit were moisten with 2 x 10 µl 0.05 M ammonium bicarbonate (ABC) and were utilized to prepare proteins from 100 µl of protein sample. Samples were spun at 14,000 rpm and mixed with 200 µl 8 M urea comprising Tris buffer. Subsequently, samples were spun and 50 mM ABC was pipetted to the samples in the filter units. After samples were spun, protein digestion was performed overnight at 37 ºC in moisten chambers using trypsin. Protein digests were spun and mixed with 50 µl 50 mM ABC. Subsequently, an *Eppendorf*^{TM} vacuum concentrator was utilized to constrict peptide solutions for 75 min at 20 ºC. Once samples were reconstituted with 40 µl of 0.1% trifluoroacetic acid (TFA), 20 µl of peptide eluate was desalted in a new tube. [9]

2.4.2. Liquid Chromatography Tandem Mass Spectrometry

All prepared samples were analyzed with the Impact II electrospray ionization quadrupole time-of-flight (QTOF) mass spectrometer. Samples were injected into the *Dionex Ultimate 3000* (Pre-column *Acclaim*^{TM} *PepMap*^{TM} *100 C18*, 100 µm x 2 cm, *nanoViper*^{TM}). The *Acclaim*^{TM} *PepMap*^{TM} *RSLC C18 nanoViper*^{TM} column with an inner diameter of 75 µm was used to separate peptides. Utilizing an increasing gradient of acetonitrile for 1.5 h and reaching 95% acetonitrile after another 10 min samples were separated and sprayed into the QTOF mass spectrometer [32]. Mass spectrometry was performed after initializing *HyStar*^{TM}. The auto

MS/MS mode with a positive ion polarity was set. Peptides were subjected to collision-induced dissociation that may vary according to peptide mass. The mass range of 150-2200 m/z was set, and the experiment was caried out with a full sensitivity resolution of 50,000. [9]

2.4.3. Proteomic Data Analysis

ProteinScape^{TM} was used for lable-free shotgun proteomic analysis. The resulting peak lists including MS/MS spectra for all samples were searched together using the mascot software against the *Swiss-Prot* protein database comprising human sequences. The *P* value of 0.05 was determined as a cutoff for significance. The protein and peptide level false discovery rate threshold of 1% was set. Mass accuracy tolerance values of 10 parts per million were set. Proteins that were identified with at least two peptides were included in the analysis [9]. Proteins were assigned to distinct divisions of the matrisome by utilizing the *MatrisomeDB* platform, which provides a computationally predicted and experimentally verified set of gene codes linked to the human matrisome [34,35].

2.4.4. SDS Page

To confirm proteomic output processed and non-processed native and fibrotic human liver samples were processed by disrupting tissues utilizing a mill and subsequently mixing samples with dithiothreitol (DTT) and SDS containing Tris-HCL buffer. To prepare proteins for SDS-page, samples were added in a 4:1 ration to the *Pierce^{TM} reducing sample buffer*. To obtain protein concentration a bicinchoninic acid (BCA) assay was performed. For this purpose, the *Pierce^{TM} BCA protein reagents A* and *B* were utilized according to specifications provided by the manufacturer. Protein concentration was measured using the microplate *reader FLUOstar OPTIMA*. A decreasing gradient of an analytical protein standard was utilized to assess protein content within the samples. Acrylamide electrophoresis gels of 1.5 mm thickness and an SDS/Tris/glycine electrophoresis running buffer (1% SDS, 25 mM Tris base, 192 mM glycine, pH 8.2) were used. Electrophoresis was run with a protein load of 100 µg for non-processed human liver samples and 30 µg for processed human liver samples. The *HiMark^{TM} Pre-stained* protein standard was applied to the gels to assess molecular weight. Loaded gels were run at an initial voltage of 100 V for the stacking gel and a voltage of 70 V for the separating gel.

2.4.5. Immunoblot Analysis

To blot proteins PVDF membranes were activated by incubating them for 5 min in 100% methanol and subsequently rinsing them with chilled blotting buffer (0.1% SDS, 20% methanol,

25 mM Tris base, 190 mM glycine, pH 8.5). Gels were stacked using the *Bio-Rad* wet tank blotting system and blotted over night at 4 ºC at 30 V. The success of the protein transfer was evaluated by immersing blots in ponceau s solution visualizing protein bands. Subsequently, blots were rinsed and blocked with either 5% skimmed milk or 5% bovine serum albumin for 1 hour. Blots blocked with 5% skimmed milk were incubated with the anti-ß-actin antibody, whereas blots blocked with 5% bovine serum albumin were incubated with the anti-collagen 6A1 antibody or the anti-TGM2 antibody. Afterwards blots were washed with polysorbate 20 containing tris buffered saline (TBST: 0.1% Tween 20, 20 mM Tris base, 150 mM NaCl, pH 7.5) and incubated with the secondary antibodies for 2 hours at room temperature. After another round of washing using TBST proteins were visualized utilizing the *Pierce^{TM} ECL* Western blotting substrate and the *ChemiDoc XRS System*.

2.5. Statistical Analysis

Statistics were performed by processing technical replicates as means. To perform group analyzes the Kruskal-Wallis test and the Dunn's multiple comparison analysis was performed. To describe spread and differences, quantitative data obtained from DNA and TAG measurements was presented by their calculated means and standard deviations. The exponentially modified protein abundance index (emPAI) [36] was used to obtain fold change ratios between different groups. The Benjamini, Krieger and Yekutieli method was used to analyze enrichment. Normalization of the quantitative results provides the opportunity to compare different samples. For all statistical analysis $P < 0.05$ was accepted as significant.

3. Results

3.1. Assessment of Created Human Liver Extracellular Matrix Scaffolds

To capture the intricacy of elements defining the human liver matrisome a high-throughput proteomic technique was utilized to determine signature patterns for long-lasting tissue specific function. To better focus the proteomic measurements on the non-cellular compartment of the human liver tissues, various decellularization and defatting strategies were drafted leading to a naturally sources ECM platform for bioengineering purposes. To assess the impact of the fabrication method and optimize the utilized technique in-depth analysis of proteomic variations were performed. The experimental design (**Figure 1A**) comprises the identification of the most suitable proceeding to fabricate human derived naturally sources ECM scaffolds (**Figure 1B**) [9].

So far, ECM scaffold fabrication methods relying on detergent-based solubilization and elimination of immunogenic products are mainly evaluated by DNA quantification [37]. Complying with currently defined specifications for successful fabrication of decellularized products, DNA content was measured quantitatively as well as qualitatively. Quantitative measurements of DNA in decellularized tissues showed a radical reduction of DNA compared to non-treated human liver samples [9]. This observation applies to not only healthy tissues treated using various decellularization strategies but also to all fibrotic and cirrhotic tissues [9]. All values comply with recommendations for the production of decellularization-based biological materials. The measured values can be observed with all quantified points in **Figure 1C**. Artificially created natural matrices were acquired by amending decellularization with various defatting strategies to eliminate macroscopic and microscopic lipids that were not removed during detergent-based treatment (**Figure 1B**). Similar results were observed for the TAG measurements presenting a thorough removal of lipids for all defatting strategies using healthy tissues as well as fibrotic and cirrhotic tissues [9]. The measured values can be observed with all quantified points in **Figure 1D**.

After obtaining quantitative evidence confirming the success of the fabrication technique, samples were evaluated by their retained tissue morphology employing histological staining. Images taken from H&E- and ORO-stained ECM scaffolds match with quantitative results from DNA and TAG assays and present an overall well-maintained microstructure and the absence of nuclei and lipids (**Figure 2**) [9]. By additionally subjecting tissue sections to immunohistochemical staining, fabricated ECM were specifically evaluated by their qualitative capabilities to maintain the tissue's basement membrane as well as the solid form building
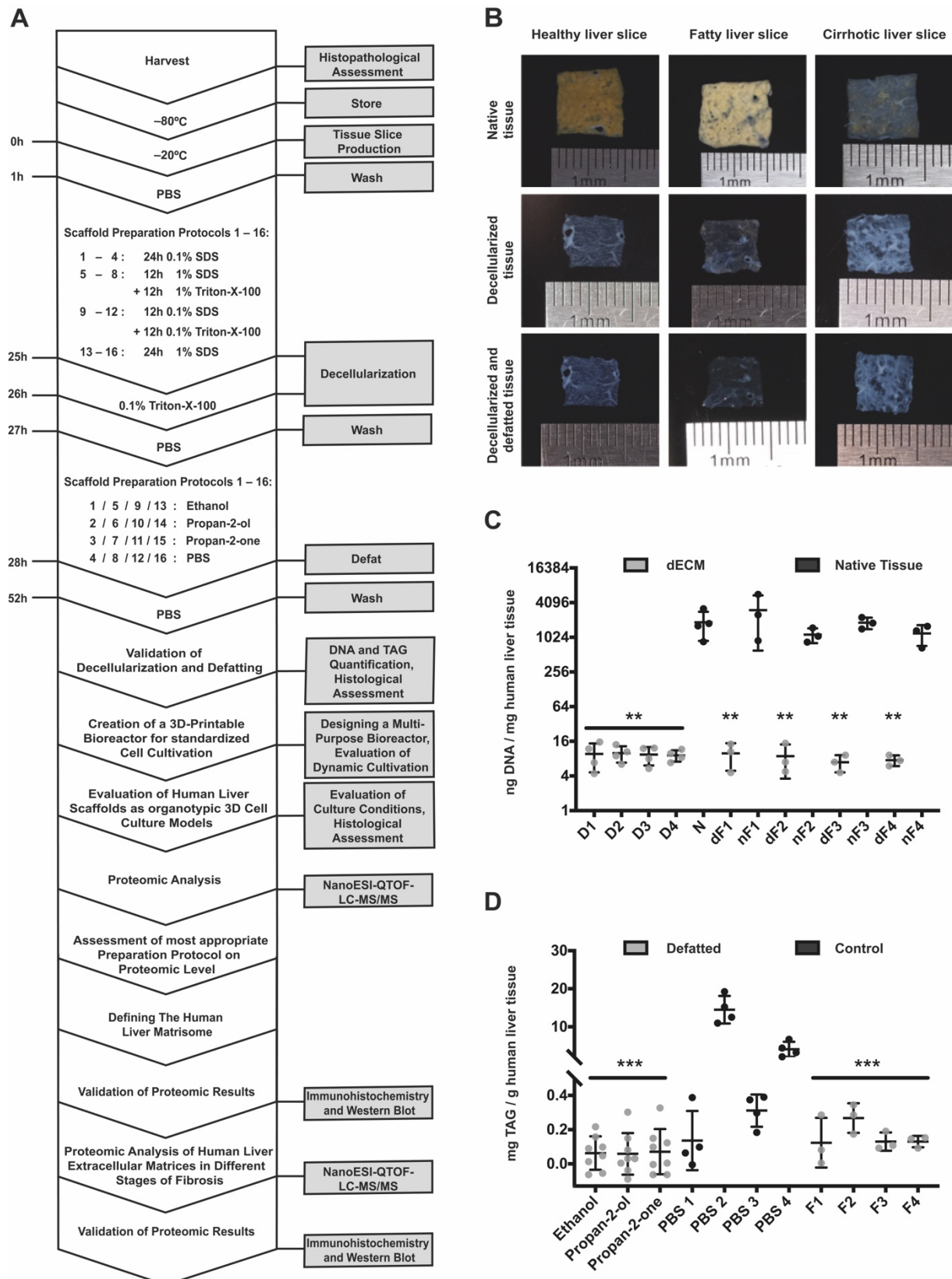
Figure 1: (A) Schematic presentation of the overall experimental design. **(B)** Human derived liver slices shown at different time points of the production process. **(C)** Quantification of DNA for all decellularization strategies and fibrotic tissue scaffolds (D1-D4: Human derived liver ECM scaffolds processed utilizing decellularization strategies 1-4; N: non-processed healthy human liver samples; dF1-dF4: Human derived liver ECM scaffolds in different stages of fibrosis; nF1-nF4: non-processed human liver samples in different stages of fibrosis). **(D)** Quantification of TAG for all defatting strategies and fibrotic tissue scaffolds (F1-F4). (**$p < 0.01$, ***$p < 0.001$). Figure adapted from [9].
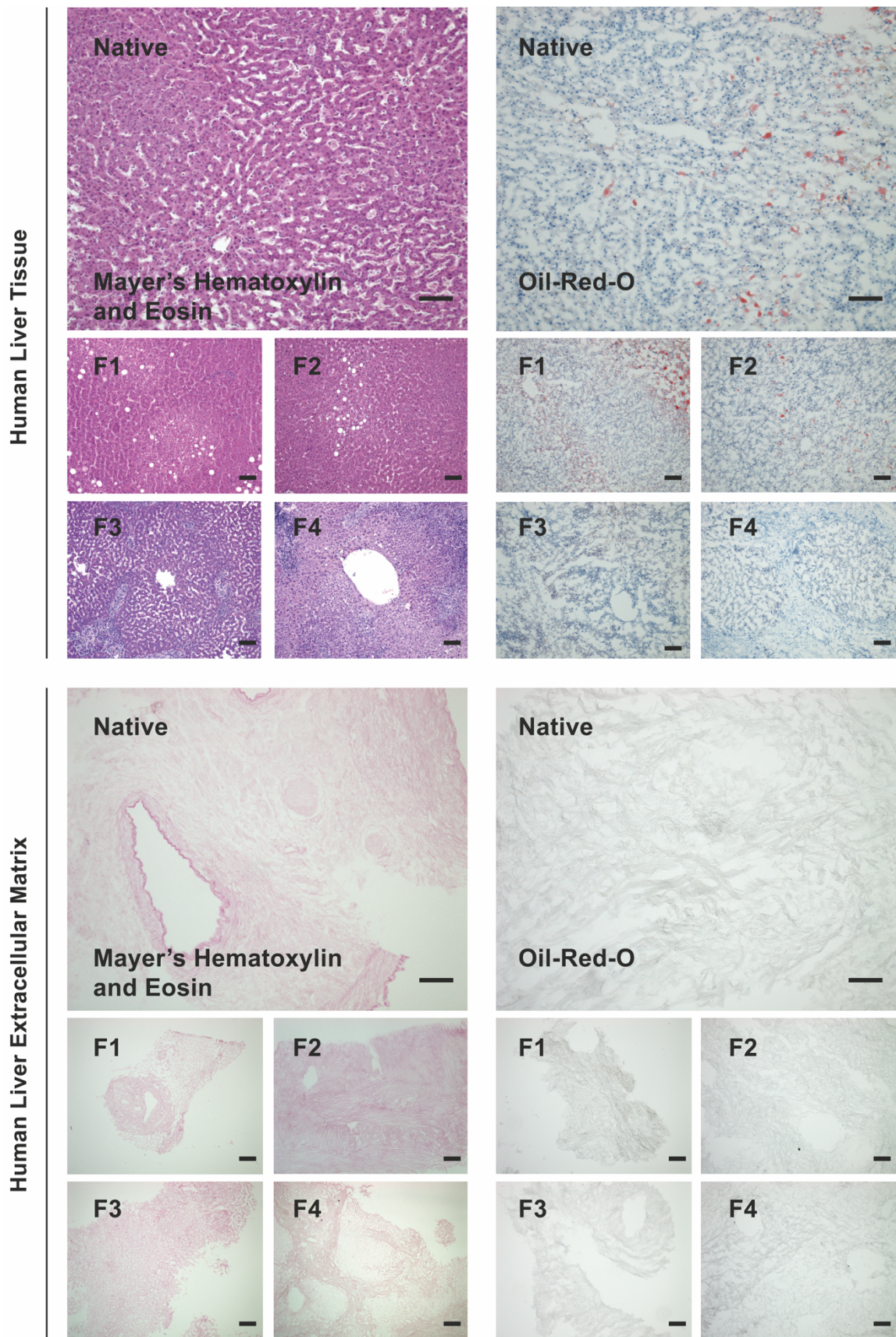
Figure 2: Mayer's Hematoxylin and Eosin and Oil-Red-O staining for non-processed human liver samples and human derived liver ECM scaffolds for healthy tissues and tissues in different stages of fibrosis (F1-F4). Scale bar: 100 μm. Figure from [9].

mesh [9]. Thus, laminin, fibronectin, collagen IV, and collagen I were visualized. The resulting fluorescence signals (**Figure 3**) demonstrate the high quality of the fabricated ECM scaffolds [9]. For better representation of the human liver ECM, **Figures 2 and 3** are amended by images obtained from non-treated human liver samples.

3.2. Evaluation of Dynamic Culture Conditions and Recellularized Human Liver Extracellular Matrix Scaffolds

The work of developing *Teburu* addressed three major objectives. First, *Teburu* provides a multi-purpose and customizable engineering platform that can be employed to analyze cell-cell and cell-matrix interactions, and thus will contribute to expand our knowledge of the various processes underlying tissue biology. Second, as a standardized and open-source system, *Teburu* is designed to provide a sustainable and easy-to-handle platform that can easily be utilized by bioengineers to address various issues in organ engineering and regenerative medicine by overcoming shortcomings in controllability and reproducibility. Lastly, by employing *Teburu* to recellularize human derived liver extracellular matrices, I aimed to gain evidence that the naturally sourced matrix scaffolds in fact do support cells and convey proliferation (**Figure 4A**).

The initial experiment employing *Teburu* (**Figures 4B, 4C**), to recellularize a human liver ECM scaffold using hMSC, aimed to determine the controllability of the cultivation system. To assess *Teburu's* capability in maintaining steady culture conditions, while operating with only small amounts of culture medium blood gas analysis were conducted for the overall dynamic recellularization time of 7 days during an experiment. During this perfusion period, *Teburu* successfully maintained solid oxygenation, electrolyte values, lactate, glucose, and pH level [32]. These data collectively provide evidence that *Teburu* as a standardized cultivation platform does ensure sufficient control for the cultivation of reseeded three-dimensional tissue scaffolds.

Naturally sourced extracellular matrices provide promising platforms to analyze cell-cell and cell-matrix interactions. Under this bioengineering paradigm, the naturally sourced extracellular matrices are expected to support cells and provide a natural environment for proliferation. Here, human liver ECM was recellularized using *Teburu* (setup shown in **Figures 4D and 4E**) and the success of recellularization was evaluated by histopathological imaging. H&E staining suggests a homogenous and well recellularization of the vertically fixed scaffold on all planes [32]. Furthermore, CD90 staining and PCNA staining were utilized to characterize cells and assess proliferation, which showed that the ECM scaffold had nearly been entirely
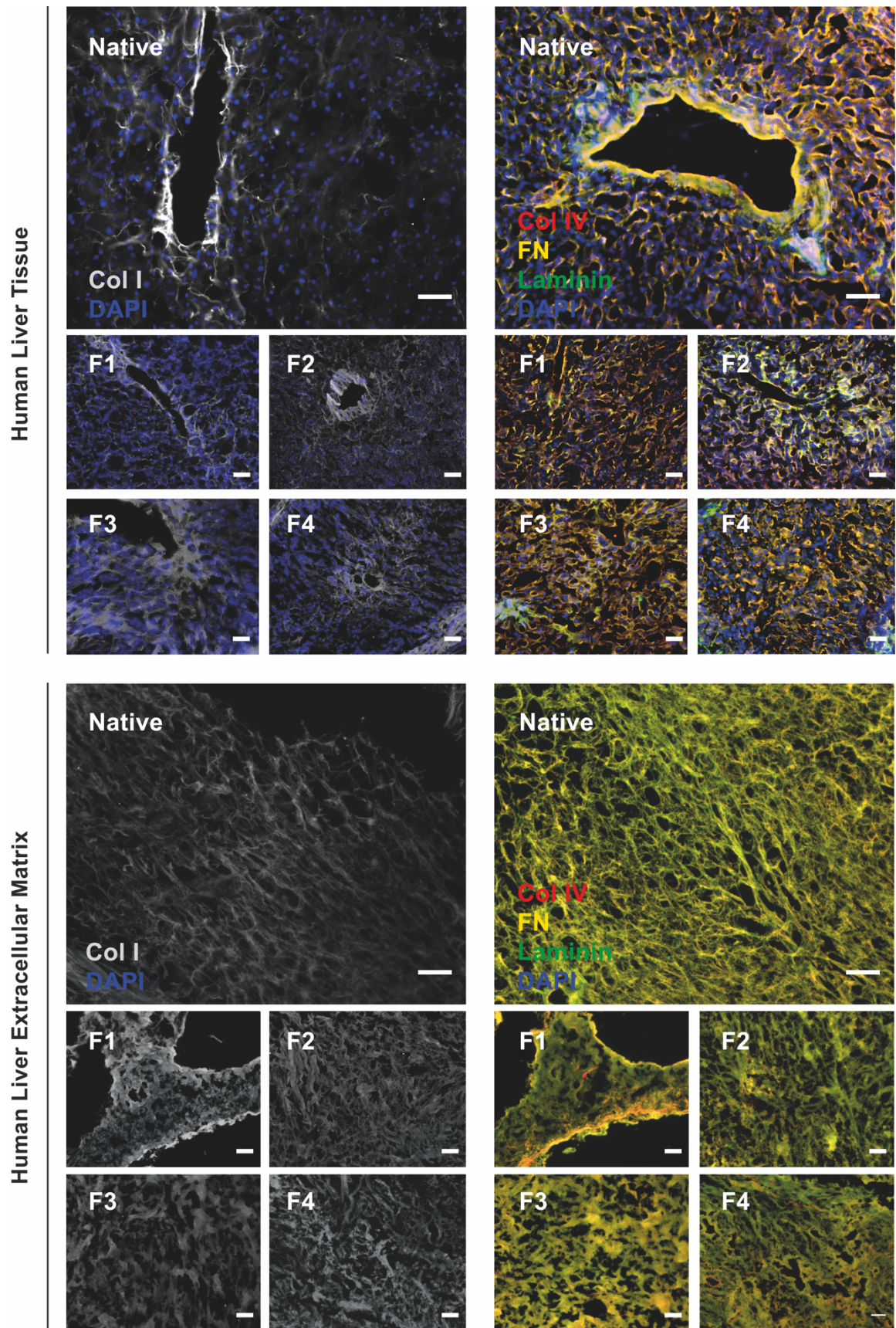
Figure 3: Immunohistochemical staining presenting the structural protein collagen I (Col I) and the basement membrane proteins laminin, fibronectin (FN) and collagen IV (Col IV) for non-processed human liver samples and human derived liver ECM scaffolds for healthy tissues and tissues in different stages of fibrosis (F1-F4). Scale bar: 50 µm. Figure from [9].
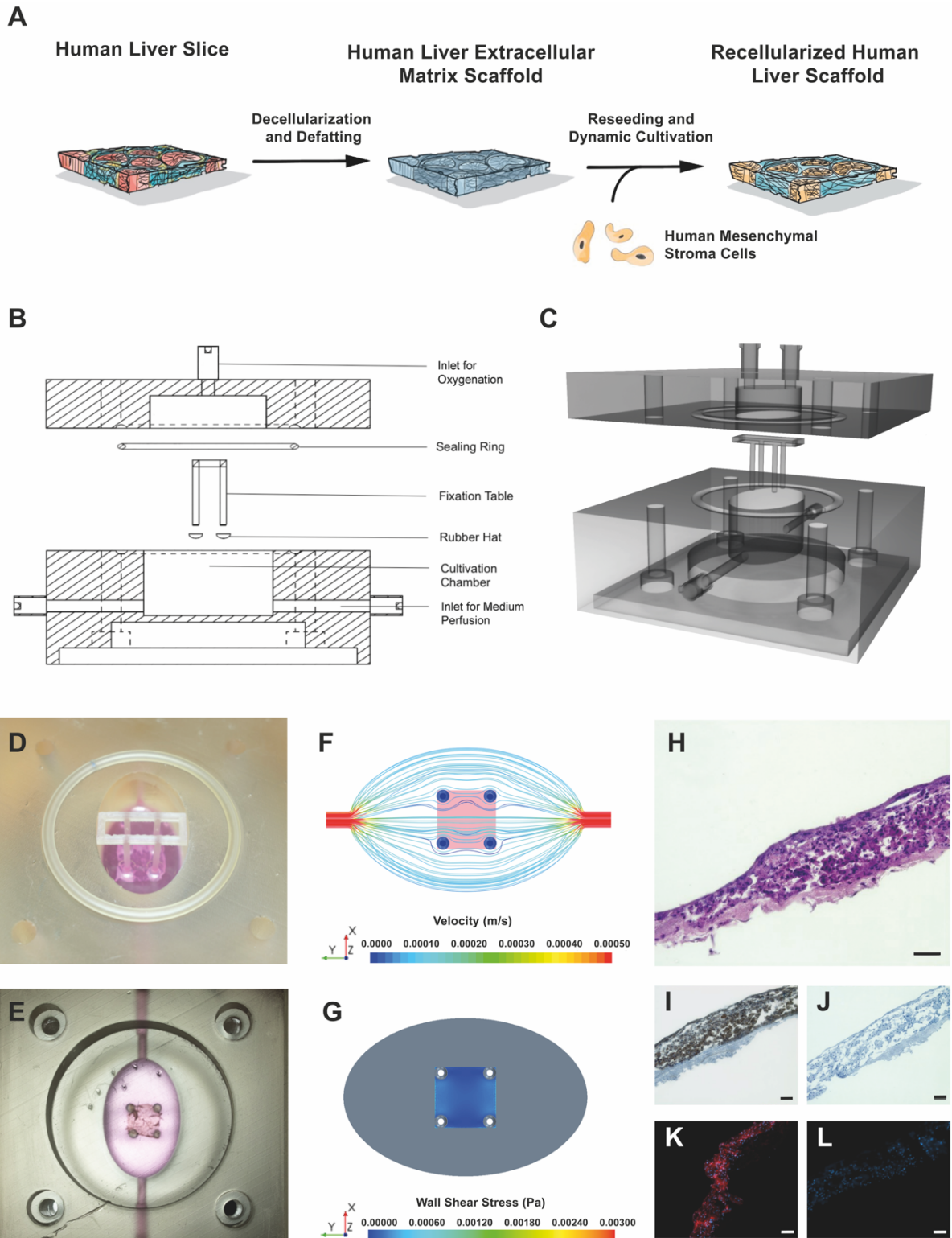
Figure 4: (A) A strategy to create a native platform to investigate biological processes. **(B)** Construction section drawing and sectional details of the bioreactor *Teburu*. **(C)** Exploded view of *Teburu*. **(D)** Fixed tissue scaffold shown from above. **E)** Fixed tissue scaffold shown from underneath the cultivation chamber. **(F)** Computational fluid dynamic analysis presenting laminar flow on the recellularized tissue scaffold. **(G)** Wall shear stress distribution on the recellularized tissue scaffold presented in Pascal. **(H)** Mayer's Hematoxylin and Eosin staining, **(I)** Proliferating-Cell-Nuclear-Antigen staining, **(J)** Proliferating-Cell-Nuclear-Antigen negative control, **(K)** CD90 staining and **(L)** CD90 negative control of a vertically sectioned recellularized human tissue scaffold presented after seven days of dynamic cultivation by employing *Teburu*. Black and white scale bars: 50 μm. Figure adapted from [32].

regrown with hMSC [32]. Immunohistochemical images resulting from the PCNA staining suggest a high number of proliferating hMSC. As simulations of the medium flow (**Figures 4F, 4G**) and the blood gas parameters already suggest, histological evaluation of cultivated human derived liver ECM scaffold confirm the system's ability to offer a necessary environment for proliferation and successful recellularization [32]. **Figures 4H – 4L** show the result of recellularization using 5 x 10^5 hMSC throughout the depth of a human derived liver scaffold for H&E, CD90 and PCNA staining [32].

3.3. Proteomic Analysis of Human Liver Extracellular Matrix Scaffolds

In contribution to biomaterial science, this thesis focuses on elucidating the proteomic compositions of the human liver matrisome to be functionalized in the fabrication of human-based matrices. For this objective, native, fibrotic and cirrhotic human derived hepatic ECM scaffolds were processed for proteomic measurements and analyzed for their distinct variances. As a first step, the most suitable technique to obtain high-quality tissue scaffolds had to be determined. Thus, all fabrication protocols were analyzed by proteomics and utilized to characterize the native human liver matrisome. The chosen technique was further utilized to capture variances in histopathologically defined stages of liver fibrosis and cirrhosis.

Utilizing the experimental workflow, a large number of proteins (774-1103) was discovered in each ECM sample underscoring the capability of the proteomic method [9]. After determining matrisome proteins and assigning them to different divisions utilizing *MatrisomeDB* provided by *Naba* et al. [34,35], the data showed 91-110 matrisome proteins for all protocols [9]. To obtain evidence about the reproducibility of the generated results for each fabrication protocol variances between different patients were assessed. The utilized experimental workflow presented that 79.51% (SD = 3.00) of all matrisome proteins overlap among replicates for all fabrication strategies [9]. By utilizing an approach provided by *Naba* et al. [34], proteins were assigned to six matrisome categories comprising proteoglycans, ECM glycoproteins, collagens, secreted factors, ECM regulators, and ECM-affiliated proteins [34]. By using this approach, 73% of the overall abundance of the human matrisome was assigned to the solid mesh of the ECM structure [9]. Accordingly, 27% of the overall abundance, which corresponds to 63 out of all 140 matrisome proteins were allocated to the fraction associated to the matrisome and thus being hold responsible for a variety of tissue specific responses of the matrisome [9]. The fabrication protocols have been observed to rather differ in regards of the number of retained matrisome-associated proteins [9]. Thus, the fabrication protocol retaining the largest number of matrisome proteins was chosen as the most suitable method to perform further analysis [9]. Consequently, the tissue scaffold fabrication protocol number 9 (**Figure 5**), which utilizes 0.1 % SDS and 0.1 % Triton-X-100 for decellularization amended by
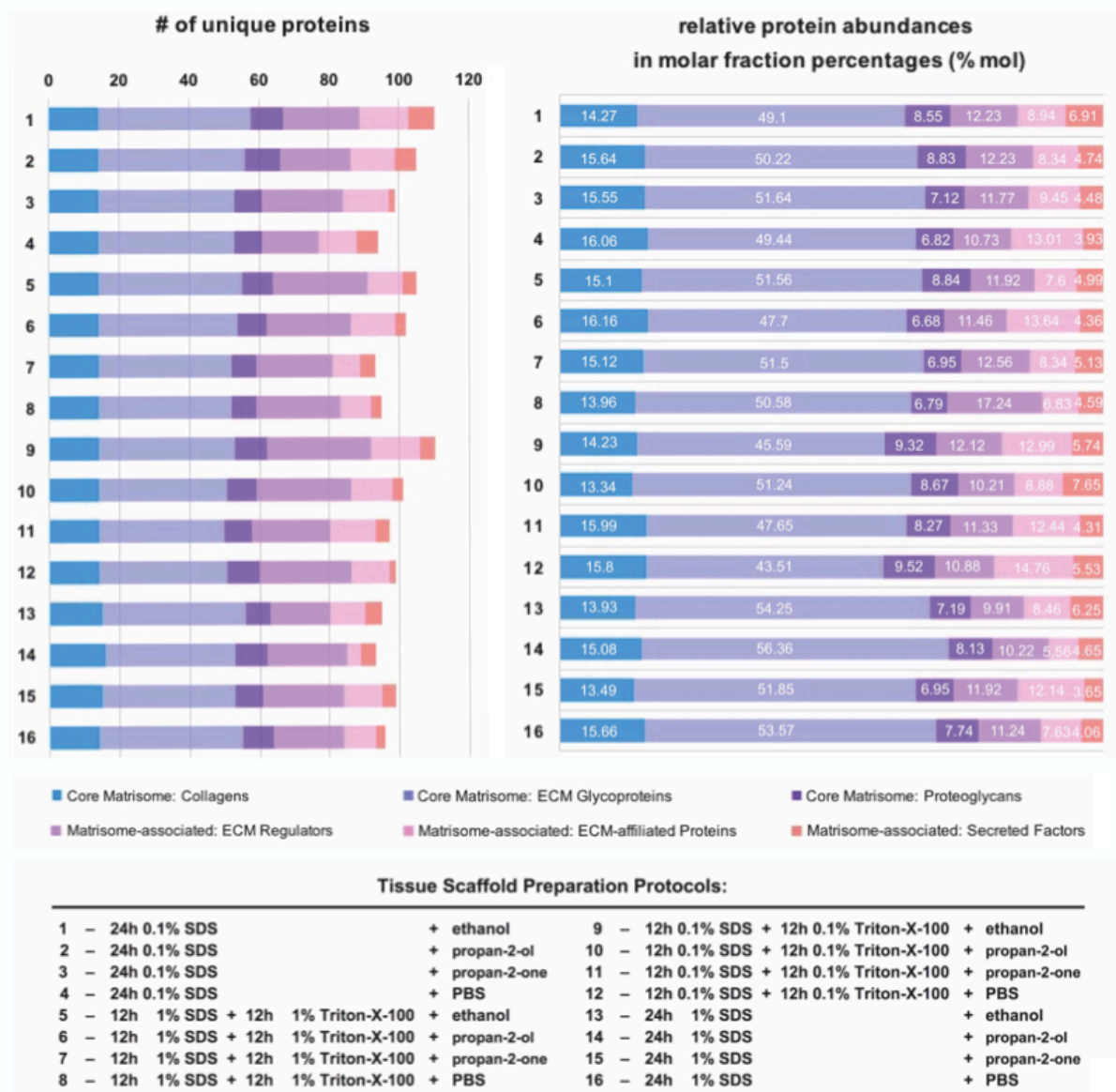
Figure 5: Diagrams presenting the absolute number of identified matrisome proteins and each matrisome sub-category's relative abundance in molar percentages (% mol) for different preparation protocols devised. Figure from [9].

defatting employing ethanol, was determined as the method of choice to produce organotypic ECM scaffolds [9]. Based on the results gained from processing 64 healthy human derived liver ECM samples, 140 proteins were defined that correspond to the native human liver matrisome [9]. These proteins are summarized in **Figure 6A**. The data was correlated to proteomic results from *Naba* et al. [38] which utilized pooled samples from human livers to obtain data on the human liver matrisome. As a result, all matrisome proteins found in this work except the plasma serin protease inhibitor and the matrix metalloprotease-9 matched their findings [9]. Since *Naba* et al. [38] had to pool collected samples for their experimental approach, due to a lack of evidence many detected proteins could not be assigned to the
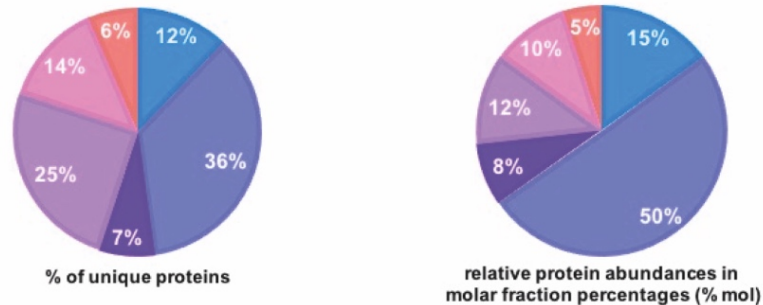
A

Core Matrisome

Collagens		ECM Glycoproteins					Proteoglycans
COL1A1	COL6A6	AEBP1	FBLN5	LAMA5	MFGE8	SRPX	ASPN
COL1A2	COL8A1	AGRN	FBN1	LAMB1	MMRN1	TGFBI	BGN
COL2A1	COL12A1	DPT	FGA	LAMB2	MMRN2	THBS1	DCN
COL3A1	COL14A1	ECM1	FGB	LAMC1	NID1	THSD4	HSPG2
COL4A1	COL17A1	EFEMP1	FGG	LGI4	NID2	TINAGL1	LUM
COL4A2	COL18A1	ELN	FN1	LTBP1	NPNT	TNC	OGN
COL5A1	COL21A1	EMILIN1	IGFALS	LTBP4	PAPLN	TNXB	PODN
COL6A1		EMILIN2	LAMA1	MATN2	PCOLCE	VTN	PRELP
COL6A2		FBLN1	LAMA3	MFAP4	POSTN	VWA1	PRG2
COL6A3		FBLN2	LAMA4	MFAP5	PXDN	VWF	PRG4

Matrisome-associated

ECM-affiliated Proteins		ECM Regulators				Secreted Factors
ANXA1	HPX	A2M	F2	MMP9	SERPINF2	ANGPTL2
ANXA11	LGALS1	ADAMTSL4	F9	PLG	SERPING1	ANGPTL6
ANXA2	LGALS3	AGT	HRG	SERPINA1	SERPINH1	CXCL12
ANXA4	LGALS4	AMBP	HTRA1	SERPINA3	TGM2	EGFL7
ANXA5	LGALS9	C17orf58	ITIH1	SERPINA4	TIMP3	INHBC
ANXA6	LGALS9B	CTSB	ITIH2	SERPINA5		INHBE
ANXA7	LMAN1	CTSD	ITIH3	SERPINA10		S100A11
C1QB	MUC5B	CTSG	ITIH4	SERPINC1		S100A8
C1QC	SEMA3B	CTSZ	KNG1	SERPIND1		S100A9
CLEC4M		F13A1	LOXL1	SERPINF1		

B

% of unique proteins: 12%, 36%, 7%, 25%, 14%, 6%

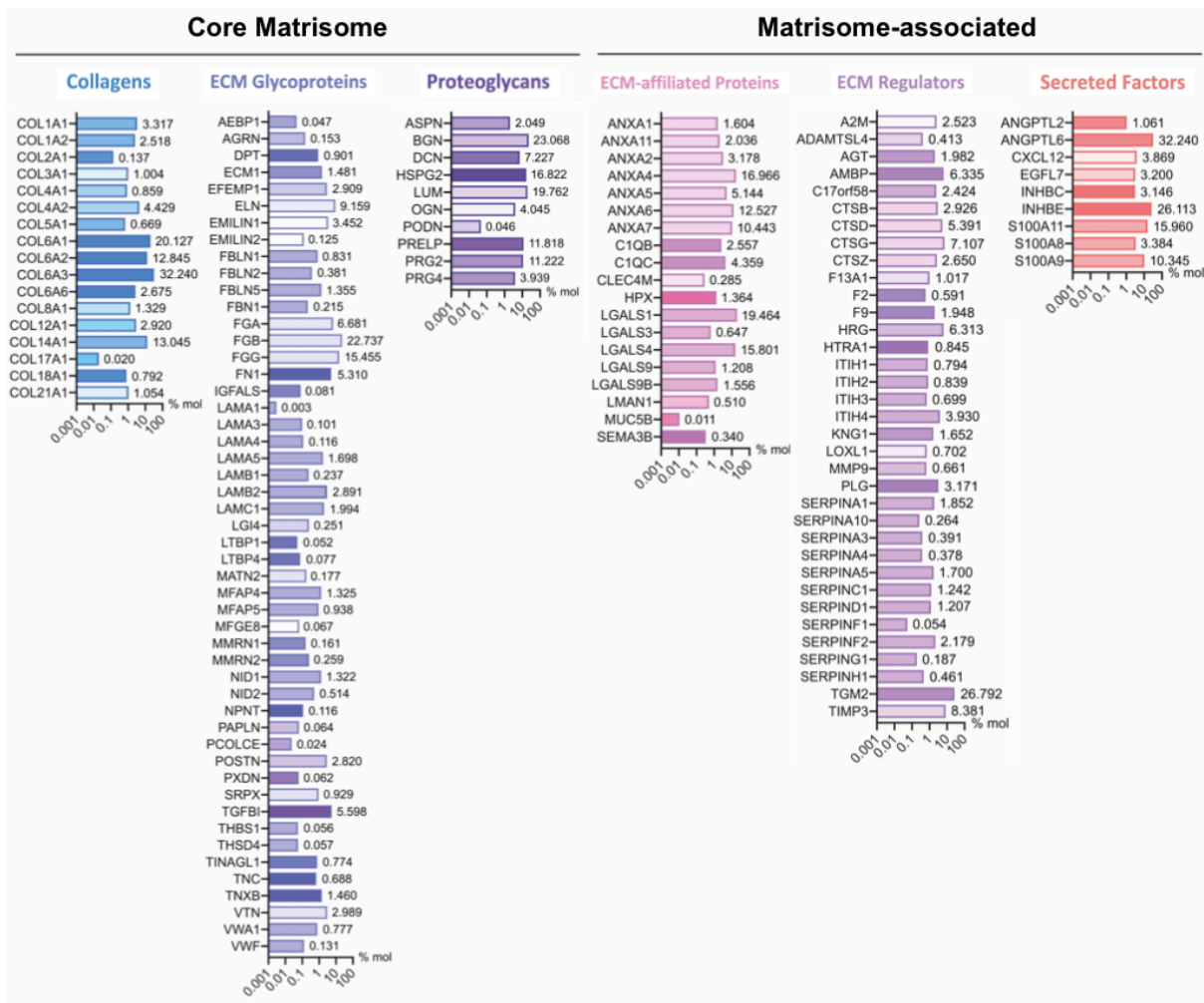relative protein abundances in molar fraction percentages (% mol): 15%, 50%, 8%, 12%, 10%, 5%

Figure 6: (A) Proteins of the healthy human liver matrisome assorted into their sub-categories. **(B)** The healthy human liver matrisome presented by the percentage of identified liver matrisome proteins and each matrisome sub-category's relative abundance in molar percentages (% mol). Figure from [9].

human liver matrisome. This work hereby amends their definition of the human liver matrisome by another 49 proteins to an overall number of 140 matrisome proteins that are shown in **Figure 6A**. [9]

For semi-quantitative characterization of matrisome proteins, the exponentially modified protein abundance index (emPAI) [36] was utilized to generate abundances and fold change ratios between groups. Out of 140 detected proteins, the core matrisome defined in this study comprises of 77 proteins, which corresponds to a molar fraction of 73% of the overall relative

abundance [9]. Thus, the core matrisome constitutes the largest number of identified proteins within the healthy human liver matrisome [9]. The overall number of native human liver matrisome proteins and their relative protein abundances is presented by different divisions in molar fractions in **Figure 6B**. Biglycan, fibrinogen gamma chain and collagen alpha-3 (VI) chain were detected with high abundances [9]. These proteins are known to provide morphological features such as mechanical stability of the ECM, cell to matrix interactions, and vascular remodeling [39-42]. Collagen VI is generally known to protect cells from oxidants and functions as an important cue for morphogenesis as well as stem cell maintenance [43]. Particularly, the collagen alpha-3 (VI) chain is of crucial importance for ECM organization by connecting the ECM to its cells [44]. Angiopoietin-related protein 6, galectin-1, annexin A5, and transglutaminase 2 (TGM2) are matrisome-associated proteins that were detected, and all contribute to a wide range of processes related to tissue signaling including growth, transduction, vascularization, and ECM cross-linkage [45-48]. The relative abundances for each native human liver matrisome protein are shown in **Figure 7**. Together, these proteins are anticipated to contribute to form, function and renewal of tissues [9].

The complex constituents of the human matrisome are responsible for tissue homeostasis and regeneration [2]. Under this paradigm, alterations in the human liver ECM will result in dysregulation and subsequent deficit in tissue function, leading to various diseases including liver fibrosis and cirrhosis [6-8] (**Figure 8A**). Thus, this dissertation further provides thorough proteomic characterization of fibrotic and cirrhotic human derived hepatic ECM scaffolds to identify potential targets for therapeutic utilization. Proteomic output generated from fibrotic and cirrhotic ECM scaffolds utilizing three biological replicates for each histopathologically defined stage of fibrosis showed that 70 matrisome proteins corresponded to all human derived hepatic ECM scaffolds [9]. Considerably, 19 native human liver matrisome proteins were absent in liver fibrosis (**Figure 8B**) [9]. Inhibin beta C chain, protein S100-A8, and hemopexin were three of these 19 proteins that are all engage in crucial regulatory processes and may be of diagnostic and therapeutic relevance in terms of determining organ functionality or graft outcome [9]. Inhibin beta C chain is involved in differentiation, proliferation and programmed cell death [49]. Protein S100-A8 regulates inflammation and protects tissues from oxidative damage [50]. Hemopexin not only regulated inflammation but is also of crucial importance in heme metabolism [51]. Furthermore, several proteins including hemicentin-1, host cell factor 1, protein Wnt-7b, and latent-transforming growth factor beta binding protein 2 were observed to be merely expressed in one of the different stages of fibrosis [9] and correspond to processes related to fiber formation, protein binding, and developmental processes [52-55]. Proteomic variances identified for healthy and fibrotic human derived liver ECM scaffolds are shown by a venn diagram presented in **Figure 8B**. For semi-quantitative comparison, emPAI

Figure 7: Proteins of the healthy human liver matrisome presented by their relative abundances in molar percentage (% mol). Figure from [9].

values [36] were used to generate abundances and fold change ratios between groups which are presented by a heatmap in **Figure 8C** for the selected fabrication protocol 9. Notably, in relation to the healthy human liver matrisome, proteins associated to the matrisome are less represented in fibrosis and comprise 31-40% of detected matrisome proteins [9]. These findings support the proposal of integrating the assessment of low abundant proteins into the interpretation of scientific data [9]. The absolute number of identified human derived liver matrisome proteins and the relative abundances assigned to different divisions of the matrisome are presented in **Figure 8D** for each histopathologically defined stage of fibrosis.

To support these findings western blot analysis was performed for three matrisome proteins. These proteins were selected from the two main divisions of the matrisome. Collagen 6A1 – a core matrisome proteins of the human liver basement membrane – that is engaged in various biological processes [43] and TGM2 – a protein associated to the matrisome – that exerts a significant role in cell regulation [45] were chosen representatively to verify the generated
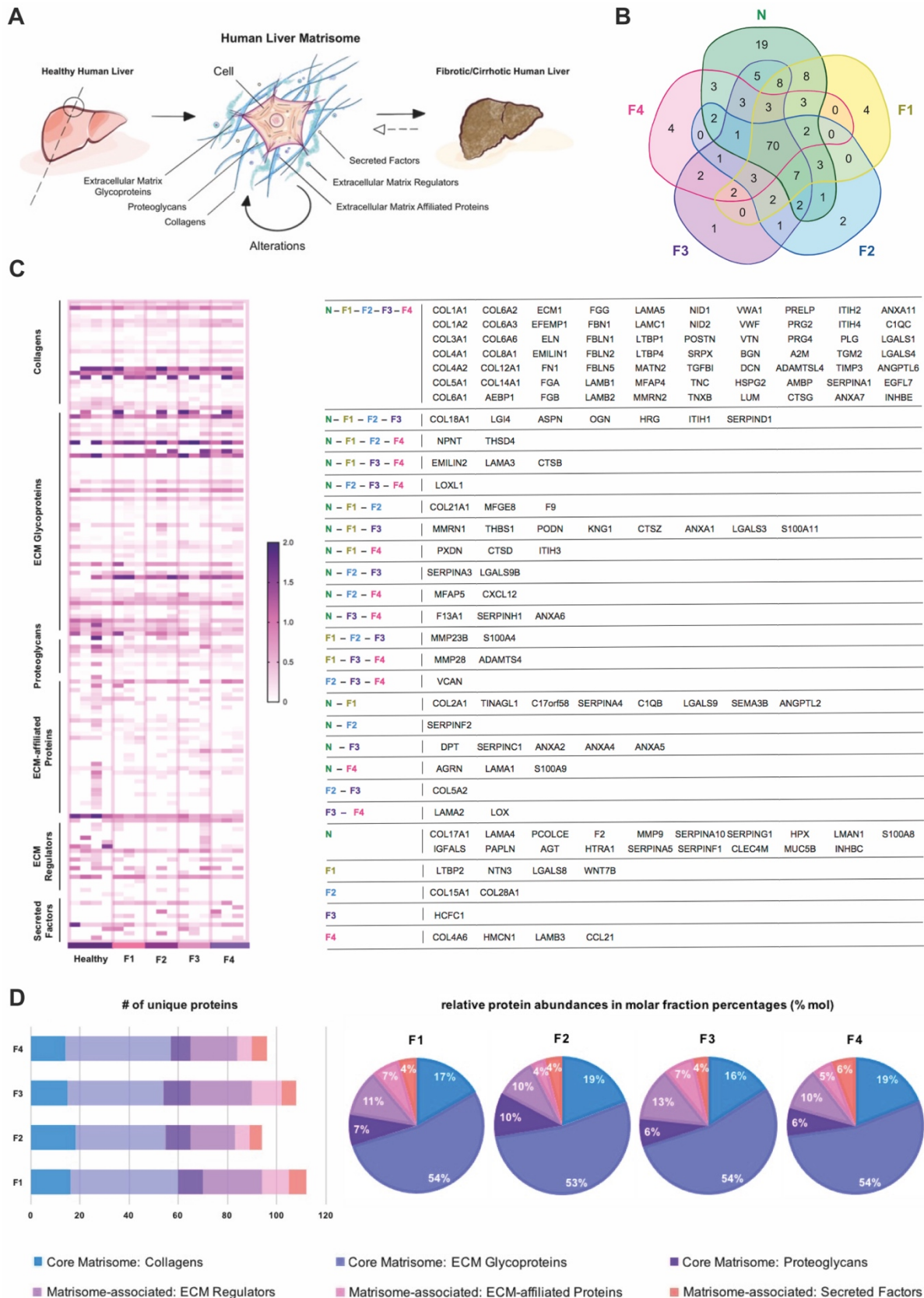
Figure 8: (A) Scheme illustrating study concept. **(B)** Venn diagram and table presenting absolute numbers of matrisome proteins identified in healthy human derived hepatic tissue scaffolds and across different stages of fibrosis. **(C)** Heatmap showing matrisome protein enrichment based on emPAI values for healthy human derived hepatic tissue scaffolds and tissues in different stages of fibrosis (F1-4). **(D)** Bar graph presenting total number of identified matrisome proteins in different stages of fibrosis (F1-4) and pie charts presenting relative matrisome protein abundances in molar percentage (% mol). Figure from [9].

results and presented matching intensities for healthy as well as fibrotic ECM samples [9]. By additionally analyzing ß-actin, which is a cellular component of living issues, western blot analysis underscored the lack of cellular material in the created ECM scaffolds [9]. For better representation of the results, these chosen proteins were also blotted and shown for non-processed human liver samples. Western blots are presented for these three selected proteins in **Figure 9**.
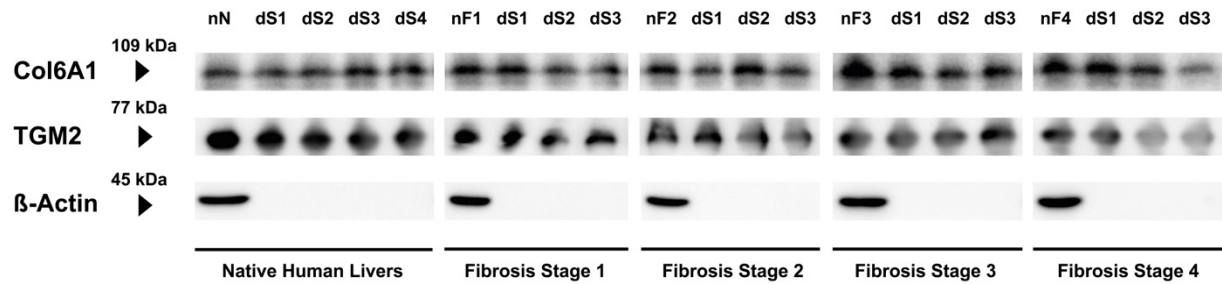
Figure 9: Western blots presenting collagen 6A1 (Col6A1), transglutaminase 2 (TGM2) and ß-actin for not processed human liver samples (nN, nF1-nF4) and human derived hepatic tissue scaffolds produced according to the preparation protocol 9 (dS1-dS3/dS4) for native tissues and tissues in different stages of fibrosis. Figure from [9].

4. Discussion

4.1. Critical Findings and Current Limitations

As liver transplantation remains the prevalent approach for the treatment of end-stage liver disease, the indisputable shortage in transplantable grafts has underlined the need for bioartificial organs. Despite the extraordinary high regenerative capacities that have provided the possibility to not only perform extensive partial liver resections but also perform partial liver resection after transplantation [5], the creation of off-the-shelf functional organ replacements yet poses a major objective in regenerative medicine. In this context, fundamental advances in digital fabrication technology and biomaterial science have led to the development of 3D printable bioinks supplemented with decellularized ECM, which inherit crucial factors for tissue survival and cell fate [13]. However, to produce biomaterials that will render long-lasting performance of bioengineered grafts, the intricacy of human matrisome constituents requires deeper exploration. Therefore, as a key objective, this thesis tackled the entirety of native human liver matrisome proteins to elucidate processes underlying tissue homeostasis and to uncover constituents which need to be considered when innovating biomaterials for the creation of non-immunogenic artificial grafts.

ECM scaffolds obtained by utilizing decellularization have dominated in the field of regenerative medicine as valuable tissues mediating regulatory behavior as well as survival of cells they host [1]. Thus, these scaffolds are vasty functionalized in organ engineering demonstrating remarkable graft outcome [56,57]. As such they present the substantial need to be further investigated. To do so, this thesis presents proteomic analysis of human derived ECM scaffolds fabricated by utilizing various drafted fabrication protocols to investigate their effects based on the anticipation that different fabrication strategies will diversely influence compositions of the matrisome [9]. Despite the wide pallet of available proteomic sample preparation techniques from which many specifically detect a delimited scope of proteins, the filter-aided sample preparation method that is reported to be a universal preparation approach [23] was chosen for this study to uncover the overall proteomic complexity of the human liver matrisome. As a result, the proteomic sample preparation method utilized in this study presented a multitude of different proteins that together highlight the potential of the employed method to disclose proteomic constituents of the human matrisome [9]. Although, the proteomic output delivered a variety of proteins that emerge with low abundances and correspond to the fraction of proteins associated to the matrisome, limitations regarding solubility and cross-linkage could be conceivable [9]. With regard to such considerations, the extensive coverage of various high/low molecular weight and high/low abundant matrisome

constituents as well as the myriad of low abundant non-matrisome proteins supports the utilized method in obtaining in-depth proteomic data from these fabricated ECM scaffolds [9]. Such capabilities are especially important to gain deeper understanding of proteins that may be depicted less dominant due to their low abundance yet convey crucial response in maintaining graft functionality [9].

Proteomic results obtained from comparing different fabrication protocols showed that proteins that are associated to the matrisome are more likely to be influenced by various fabrication methods rather than the actual core division of the matrisome [9]. This should be taken into consideration when utilizing decellularization and defatting techniques to fabricate naturally derived ECM scaffolds to be further functionalized in the development of bioartificial organs. Based on the obtained proteomic output, it can be concluded that matrisome-associated ECM proteins comprise the more dynamic division of human matrices [9]. Thus, various ECM fabrication protocols considerably vary regarding the ensemble of retained proteins associated to the matrisome [9]. The most suitable method for the creation of ECM scaffolds thus retains the largest number of proteins corresponding to the matrisome [9]. Moreover, taking the vast applications of decellularized ECM scaffolds into consideration, the large number of low-abundant non-matrisome proteins from which several may elicit immunogenic responses despite their low-abundances, implies the significance of utilizing proteomic techniques to investigate potential immunogenicity of biomaterials containing decellularization-based ECM [9].

4.2. Future Directions in Biomaterial Science and Organ Engineering

A persistent challenge in creating functional biomaterials for non-immunogenic bioartificial organ replacements lies in developing a suitable environment that will maintain functionality and integration of grafts. To achieve this, decellularization was utilized to produce natural ECM scaffolds inheriting bioactive features necessary for cell survival and regeneration [1]. Nevertheless, a variety of non-matrisome proteins which will be retained in these matrices although in low abundances can potentially elicit immune responses and thus may pose a threat to the performance of transplanted grafts [9]. Underlying processes that would lead to such reactions and the extent to which such factors may harm engraftment will require further investigation. Although, such observations have been documented in other reports [11,58], questions related to the utilization of these decellularized ECM scaffolds in creating non-immunogenic grafts and their potential influence in the long run still need to be addressed. The production of novel biomaterials capable of cell encapsulation and long-lasting organotypic functionality should involve the overall constituents and relative abundances of proteins corresponding to the human matrisome, while relinquishing on an involvement of non-

matrisome proteins that are inevitably retained during decellularization and may be unfavorable upon transplantation [9]. The development of synthetically created biomaterials that are made based on their human analogues and the utilization of bioprinting technologies could be conceivable strategies tackling potential immunogenicity [9]. This thesis hereby proposes the concept of creating novel biomaterials by functionalizing information regarding the human matrisome that can be combined with digital fabrication techniques to create bioartificial grafts. Novel non-immunogenic bio-inks should be produced by combining proteins presented in this study that will involve crucial cues for liver scaffold functionality [9]. For this purpose, this thesis provides in-depth analysis of human liver matrisome proteins [9]. These proteins are expected to mediate long-lasting performance of bioartificial organs and therefore require further research [9].

4.3. Outlook on Clinical Applications

The tightly regulated native human proteome is responsible for essential biological processes maintaining tissue function and regeneration. Changes to the constituents of the native human proteome are widely acknowledged to lead to diseases including liver fibrosis and cirrhosis [6-8]. To understand human tissues and the way they respond to stress and damage, and ultimately the reasons underlying the emergence of diseases, organotypic human tissue scaffolds provide personalized platforms to investigate diagnostic and therapeutic opportunities. By presenting in-depth analysis of healthy, fibrotic and cirrhotic human liver ECM scaffolds and introducing *Teburu* as a multi-purpose and openly accessible investigation platform, this thesis sets the foundation to further functionalize the presented data for a broad pallet of bioengineering approaches. Conceivable future objectives in medicine may range from the development of novel therapeutics, to programable and responsive scaffolds in the scope of controlled medical devices, to the creation of novel biomaterials enhancing self-healing capabilities. The experimental workflow presented provides a customizable platform to investigate tissues of different origin and shall further expand our view on biological matrices and the ways we may functionalize them to pave new paths to maintain health and tackle diseases.

6. References

[1]   G.S. Hussey, J.L. Dziki, S.F. Badylak, Extracellular matrix-based materials for regenerative medicine, Nat. Rev. Mater. 3 (2018) 159–173.

[2]   R.O. Hynes, K.M. Yamada, Extracellular Matrix Biology, Cold Spring Harbor Perspectives in Biology, Cold Spring Harbor Laboratory Press: Cold Spring Harbor, NY, 2011.

[3]   T. Rozario, D.W. DeSimone, The extracellular matrix in development and morphogenesis: a dynamic view, Dev. Biol. 341 (2010) 126–140.

[4]   C. Frantz, K.M. Stewart, V.M. Weaver, The extracellular matrix at a glance, J. Cell Sci. 123 (2010) 4195–4200.

[5]   J.M.O. Pohl, N. Raschzok, D. Eurich, M. Pflüger, L. Wiering, A. Daneshgar, T. Dziodzio, M. Jara, B. Globke, I.M. Sauer, M. Bieble, G. Lurje, W. Schöning, M. Schmelzle, F. Tacke, J. Pratschke, P. Ritschl, R. Öllinger, Outcomes of liver resections after liver transplantation at a high-volume hepatobiliary center, J. Clin. Med. 9 (2020) 3685.

[6]   C. Bonnans, J. Chou, Z. Werb, Remodeling the extracellular matrix in development and disease, Nat. Rev. Mol. Cell Biol. 15 (2014) 786-801.

[7]   T.R. Cox, J.T. Erler, Remodeling and homeostasis of the extracellular matrix: implications for fibrotic diseases and cancer, Dis. Model Mech. 4 (2011) 165-178.

[8]   P. Bedossa, V. Paradis, Liver extracellular matrix in health and disease, J Pathol 200 (2003) 504-515.

[9]   Daneshgar A, Klein O, Nebrich G, Weinhart M, Tang P, Arnold A, Ullah I, Pohl J, Moosburner S, Raschzok N, Strücker B, Bahra M, Pratschke J, Sauer IM, Hillebrandt KH. The human liver matrisome - Proteomic analysis of native and fibrotic human liver extracellular matrices for organ engineering approaches. Biomaterials. 257 (2020) 120247.

[10]   K.H. Hillebrandt, H. Everwien, N. Haep, E. Keshi, J. Pratschke, I.M. Sauer, Strategies based on organ decellularization and recellularization, Transpl. Int. 32 (2019) 571–585.

[11]   Q. Li, B.E. Uygun, S. Geerts, S. Ozer, M. Scalf, S.E. Gilpin, H.C. Ott, M.L. Yarmush, L.M. Smith, N.V. Welham, B.L. Frey, Proteomic analysis of naturally-sourced biological scaffolds, Biomaterials 75 (2016) 37–46.

[12]   I. Matai, G. Kaur, A. Seyedsalehi, A. McClinton, C.T. Laurencin, Progress in 3D bioprinting technology for tissue/organ regenerative engineering, Biomaterials 226 (2019) 119536.

[13]   W. Han, N.K. Singh, J.J. Kim, H. Kim, B.S. Kim, J.Y. Park, J. Jang, D. Cho, Directed differential behaviors of multipotent adult stem cells from decellularized tissue/ organ extracellular matrix bioinks, Biomaterials 224 (2019) 119496.

[14]   M.M. De Santis, H.N. Alsafadi, S. Tas, D.A. Bölükbas, S. Prithiviraj, I.A.N. Da Silva, M. Mittendorfer, C. Ota, J. Stegmayr, F. Daoud, M. Königshoff, K. Swärd, J.A. Wood, M. Tassieri, P.E. Bourgine, S. Lindstedt, S. Mohlin, D.E. Wagner, Extracellular-Matrix-Reinforced Bioinks for 3D Bioprinting Human Tissue, Adv. Mater. 33 (2021) 2005476.

[15]   A. Pandey, M. Mann, Proteomics to study genes and genomes, Nature 405 (2000) 837–846.

[16]   R. Aebersold, M. Mann, Mass spectrometry-based proteomics, Nature 422 (2003) 198–207.

[17]   G.S. Omenn, L. Lane, C.M. Overall, I.M. Cristea, F.J. Corrales, C. Lindskog, Y. Paik, J.E. Van Eyk, S. Liu, S.R. Pennington, M.P. Snyder, M.S. Baker, N. Bandaira, R. Aebersold, Research on the human proteome reaches a major milestone: >90% of predicted human proteins now credibly detected, according to HUPO human proteome project, J Proteome Res. 12 (2020) 4735-4746.

[18]   Y. Zhang, B.R. Fonslow, B. Shan, M. Baek, J.R. Yates III, Protein analysis by shotgun/bottom-up proteomics, Chem Rev. 4 (2013) 2343-2394.

[19]   D.A. Wolters, M.P. Washburn, J.R. Yates III, An automated multidensional protein identification technology for shotgun proteomics, Anal Chem. 23 (2001) 5683-5690.

[20]   A.J. Link, J. Eng, D.M. Schieltz, E. Carmack, G.J. Mize, D.R. Morris, B.M. Garvik, J.R. Yates III, Direct analysis of protein complexes using mass spectrometry, Nat Biotechnol. 7 (1999) 676-682.

[21]   R. Aebersold, M. Mann, Mass-spectrometric exploration of proteome structure and function, Nature 537 (2016) 347–355.

[22]   K.C. Hansen, L. Kiemele, O. Maller, J. O'Brien, A. Shankar, J. Fornetti, P. Schedin, An in-solution ultrasonication-asissted digestion method for improved extracellular matrix proteome coverage, Mol. Cell. Proteomics 8 (2009) 1648–1657.

[23]   J.R. Wisniewski, A. Zougman, N. Nagaraj, M. Mann, Universal sample preparation method for proteome analysis, Nat. Methods 6 (2009) 359–362.

[24]   B. Grigoryan, S.J. Paulsen, D.C. Corbett, D.W. Sazer, C.L. Fortin, A.J. Zaita, P.T. Greenfield, N.J. Calafat, J.P. Gounley, A.H. Ta, F. Johansson, A. Randles, J.E. Rosenkrantz, J.D. Louis-Rosenberg, P.A. Galie, K.R. Stevens, J.S. Miller, Multivascular networks and functional intravascular topologies within biocompatible hydrogels, Science 364 (2019) 458-464.

[25] A. Lee, A.R. Hudson, D.J. Shiwarski, J.W. Tashman, T.J. Hinton, S. Yerneni, J.M. Bliley, P.G. Campbell, A.W. Feinberg, 3D bioprinting of collagen to rebuild components of the human heart, Science 365 (2019) 482-487.

[26] A. Porzionato, E. Stocco, S. Barbor, F. Grandi, V. Macchi, R. De Caro, Tissue-engineered grafts from human decellularized extracellular matrices: a systematic review and future perspectives, Int. J. Mol. Sci. 19 (2018) 4117.

[27] S. Sasikumar, S. Chameettachal, B. Cromer, F. Pati, P. Kingshott, Decellularized extracellular matrix hydrogels–cell behavior as a function of matrix stiffness, Curr. Opin. Biomed. Eng. 10 (2019) 123-133.

[28] G. Agmon, K.L. Christman, Controlling stem cell behavior with decellularized extracellular matrix scaffolds, Curr Opin Solid State Mater Sci. 20 (2016) 193-201.

[29] T. Bruegmann, D. Malan, M. Hesse, T. Beiert, C.J. Fruegemann, B.K. Fleischmann, P. Sasse, Optogenetic control of heart muscle in vitro and in vivo, Nat Methods 7 (2010) 897-900.

[30] E. Kwon, H.Y. Joung, S.M. Liu, S.C. Chua Jr., G.J. Schwartz, Y.H. Jo, Optogenetic stimulation of the liver-projecting melanocortinergic pathway promotes hepatic glucose production, Nat Commun 11 (2020) 6295.

[31] I.Y. Choi, H.T. Lim, A. Huynh, J. Schofield, H.J. Cho, H. Lee, P. Anderson, J.H. Shin, W.D. Heo, S.H. Hyun, Y.J. Kim, Y. Oh, H. Kim, G. Lee, Novel culture system via wireless controllable optical stimulation of the FGF signaling pathway for human and pig pluripotency, Biomaterials. 269 (2021) 120222.

[32] A. Daneshgar, P. Tang, C. Remde, M. Lommel, S. Moosburner, U. Kertzscher, O. Klein, M. Weinhart, J. Pratschke, I.M. Sauer, K.H. Hillebrandt, Teburu - Open source 3D printable bioreactor for tissue slices as dynamic three-dimensional cell culture models, Artif. Organs 43 (2019) 1035–1041.

[33] M. Israelowitz, B. Weyand, S. Rizvi, P.M. Vogt, H.P. von Schroeder, Development of a laminar flow bioreactor by computational fluid dynamics, J Healthc Eng. 3 (2012) 455-476.

[34] A. Naba, K.R. Clauser, H. Ding, C.A. Whittaker, S.A. Carr, R.O. Hynes, The extracellular matrix: tools and insights for the "omics" era, Matrix Biol. 49 (2016) 10–24.

[35] A. Naba, K.R. Clauser, S. Hoersch, H. Liu, S.A. Carr, R.O. Hynes, The matrisome: in silico definition and in vivo characterization by proteomics of normal and tumor extracellular matrices, Mol. Cell. Proteomics 11 (2012), 014647M111.

[36] Y. Ishihama, Y. Oda, T. Tabata, T. Sato, T. Nagasu, J. Rappsilber, M. Mann, Exponentially modified protein abundance index (emPAI) for estimation of absolute protein amount in proteomics by the number of sequenced peptides per protein, Mol. Cell. Proteomics 4 (2005) 1265–1272.

[37] P.M. Capro, T.W. Gilbert, S.F. Badylak, An overview of tissue and whole organ decellularization processes, Biomaterials 32 (2011) 3233–3243.

[38] A. Naba, K.R. Clauser, C.A. Whittaker, S.A. Carr, K.K. Tanabe, R.O. Hynes, Extracellular matrix signatures of human primary metastatic colon cancers and their metastases to liver, BMC Canc. 14 (2014) 518–529.

[39] L.R. Languino, J. Plescia, A. Duperray, A.A. Brian, E.F. Plow, J.E. Geltosky, D. C. Altieri, Fibrinogen mediates leukocyte adhesion to vascular endothelium through an ICAM-1-dependent pathway, Cell 73 (1993) 1423–1434.

[40] U. Sen, N. Tyagi, P.K. Patibandla, W.L. Dean, S.C. Tyagi, A.M. Roberts, D. Lominadze, Fibrinogen-induced endothelin-1 production from endothelial cells, Am. J. Physiol. Cell Physiol. 296 (2009) C840–C847.

[41] M. Myren, D.J. Kirby, M.L. Noonan, A. Maeda, R.T. Owens, S. Ricard-Blum, V. Kram, T.M. Kilts, M.F. Young, Biglycan potentially regulates angiogenesis during fracture repair by altering expression and function of endostatin, Matrix Biol. 52–54 (2016) 141–150.

[42] M.V. Nastase, M.F. Young, L. Schaefer, Biglycan a multivalent proteoglycan providing structures and signals, J. Histochem. Cytochem. 60 (2012) 963–975.

[43] M. Cescon, F. Gattazzo, P. Chen, P. Bonaldo, Collagen VI at a glance, J. Cell Sci.128 (2015) 3525–3531.

[44] S.R. Lamande, M. Mörgelin, N.E. Adams, C. Selan, J.M. Allen, The C5 domain of the collagen VI a3(VI) chain is critical for extracellular microfibril formation and is present in the extracellular matrix of cultured cells, J. Biol. Chem. 281 (2006) 16607–16614.

[45] A. Maeda, T. Nishino, R. Matsunaga, A. Yokoyama, H. Suga, T. Yagi, H. Konishi, Transglutaminase-mediated cross-linking of WDR54 regulates EGF receptor signaling, Biochim. Biophys. Acta Mol. Cell Res. 1866 (2019) 285–295.

[46] A. Bruneel, V. Labas, A. Mailloux, S. Sharma, N. Royer, J. Vinh, P. Pernet, M. Vaubourdolle, B. Baudin, Proteomics of human umbilical vein endothelial cells applied to etoposide-induced apoptosis, Proteomics 5 (2005) 3876–3884.

[47] N.G. Than, R. Romero, M. Goodman, A. Weckle, J. Xing, Z. Dong, Y. Xu, F. Tarquini, A. Szilagyi, P. Gal, Z. Hou, A.L. Tarca, C.J. Kim, J.S. Kim, S. Haidarian, M. Uddin, H. Bohn, K. Benirschke, J. Santolaya-Forgas, L.I. Grossman, O. Erez, S. S. Hassan, P. Zavodszky, Z. Papp, D.E. Wildman, A primate subfamily of galectins expressed at the maternal-fetal interface that promote immune cell death, Proc. Natl. Acad. Sci. U.S.A. 106 (2009) 9731–9736.

[48] C. Carbone, G. Piro, V. Merz, F. Simionato, R. Santoro, C. Zecchetto, G. Tortora, D. Melisi, Angiopoietin-like proteins in angiogenesis, inflammation and cancer, Int. J. Mol. Sci. 19 (2018) 431.

[49] K. Frost, K. Seir, A. Lackner, M. Grusch, B. Grasl-Kraupp, R. Schulte-Hermann and C. Rodgarkia-Dara, Inhibin/activin expression in human and rodent liver: subunits α and ßB as new players inhuman hepatocellular carcinoma?, Br J Cancer. 104 (2011) 1303-1312.

[50] S. Berthier, M.V. Nyugen, A. Baillet, M.A. Hograindleur, M.H. Paclet, B. Polack, F. Morel, Molecular interface of S100A8 with cytochrome b558 and NADPH oxidase activation, PloS One 7 (2012) e40277.

[51] T. Lin, D. Maita, S.R. Thundivalappil, F.E. Riley, J. Hambsch, L.J. Van Marter, H.A. Christou, L. Berra, S. Fagan, D.C. Christiani, H.S. Warren, Hemopexin in severe inflammation and infection: mouse models and human diseases, Crit Care. 19 (2015) 166.

[52] M. Eubelen, N. Bostaille, P. Cabochette, A. Gauquier, P. Tebabi, A.C. Dumitru, M. Koehler, P. Gut, D. Alsteens, D.Y.R. Stainier, A. Garcia-Pino, B. Vanhollebeke, A molecular mechanism for Wnt ligand-specific signaling, Science 361 (2018) 6403.

[53] R. Öklü, R. Hesketh, The latent transforming growth factor ß binding protein (LTBP family, Biochem. J. 352 (2000) 601–610.

[54] X. Xu, M. Xu, X. Zhou, O.B. Jones, E. Moharomd, Y. Pan, G. Yan, D.D. Anthony, W.B. Isaacs, Specific structure and unique function define the hemicentin, Cell Biosci. 3 (2013) 27.

[55] P. Zhou, Z. Wang, X. Yuan, C. Zhou, L. Liu, X. Wan, F. Zhang, X. Ding, C. Wang, S. Xiong, Z. Wang, J. Yuan, Q. Li, Y. Zhang, Mixed lineage leukemia 5 (MLL5) protein regulates cell cycle progression and E2F1-responsive gene expression via association with host cell factor-1 (HCF-1), J. Biol. Chem. 288 (2013) 17532–17543.

[56] A. Citro, P.T. Moser, E. Dugnani, T.K. Rajab, X. Ren, D. Evangelista-Leite, J.M. Charest, A. Paleso, B.K. Podesser, F. Maneti, S. Pellegrini, L. Piemonti, H. Ott, Biofabrication of a vascularized islet organ for type 1 diabetes, Biomaterials 199 (2019) 40-51.

[57] K. Takeishi, A. Collin de l'Hortet, Y. Wang, K. Handa, J. Guzman-Lepe, K. Matsubara, K. Morita, S. Jang, N. Haep, R.M. Florentino, F. Yuan, K. Fukumitsu, K. Tobita, W. Sun, J. Franks, E.R. Delgado, E.M. Shapiro, N.A. Fraunhoffer, A.W. Duncan, H. Yagi, T. Mashimo, I.J. Fox, A. Soto-Gutierrez, Assembly and fuction of a bioengineering human liver for transplantation generated solely from induced pluripotent stem cells, Cell Rep. 9 (2020) 107711.

[58] F. Ma, D.M. Tremmel, Z. Li, C.B. Lietz, S.D. Sackett, J.S. Odorico, L. Li, In depth quantification of extracellular matrix proteins from human pancreas, J. Proteome Res. 18 (2019) 3156–3165.

Statutory Declaration

"I, Assal Daneshgar, by personally signing this document in lieu of an oath, hereby affirm that I prepared the submitted dissertation on the topic 'Proteomic analysis of the native and fibrotic human liver matrisome for organ engineering / Proteomische Analyse des nativen und fibrotischen humanen Lebermatrisoms für Organ Engineering', independently and without the support of third parties, and that I used no other sources and aids than those stated.

All parts which are based on the publications or presentations of other authors, either in letter or in spirit, are specified as such in accordance with the citing guidelines. The sections on methodology (in particular regarding practical work, laboratory regulations, statistical processing) and results (in particular regarding figures, charts and tables) are exclusively my responsibility.

Furthermore, I declare that I have correctly marked all of the data, the analyses, and the conclusions generated from data obtained in collaboration with other persons, and that I have correctly marked my own contribution and the contributions of other persons (cf. declaration of contribution). I have correctly marked all texts or parts of texts that were generated in collaboration with other persons.

My contributions to any publications to this dissertation correspond to those stated in the below joint declaration made together with the supervisor. All publications created within the scope of the dissertation comply with the guidelines of the ICMJE (International Committee of Medical Journal Editors; www.icmje.org) on authorship. In addition, I declare that I shall comply with the regulations of Charité – Universitätsmedizin Berlin on ensuring good scientific practice.

I declare that I have not yet submitted this dissertation in identical or similar form to another Faculty.

The significance of this statutory declaration and the consequences of a false statutory declaration under criminal law (Sections 156, 161 of the German Criminal Code) are known to me."

Assal Daneshgar   Berlin, 08.07.2021

Declaration of Author's Contribution

Assal Daneshgar contributed the following to the below listed publications:

Publication 1: Daneshgar A, Klein O, Nebrich G, Weinhart M, Tang P, Arnold A, Ullah I, Pohl J, Moosburner S, Raschzok N, Strücker B, Bahra M, Pratschke J, Sauer IM, Hillebrandt KH. The human liver matrisome - Proteomic analysis of native and fibrotic human liver extracellular matrices for organ engineering approaches. Biomaterials. 2020 Oct;257:120247.

My Contribution in Detail: As the lead author of the publication, I contributed an overall share of 80% to all aspect of this study, including conceptualization, planning, devising and employing all methods and experiments, generating, analyzing, validating and interpreting all data and results as well as writing and revising the manuscript. During my doctoral thesis, I came to understand the importance of the human proteomic landscape and their essential role in the creation of functional organ replacements. Thus, I set up the idea of defining the human liver matrisome for approaches in the field of organ engineering. The concept of assessing the effects of different tissue scaffold preparation protocols on matrisome compositions was set up together with Dr. med. Karl Herbert Hillebrandt. Throughout this work, I was responsible for the acquisition and handling of samples and was also responsible for the creation of human liver slices. I devised and employed the preparation protocols (decellularization and defatting of human liver slices) for the creation of human liver extracellular matrix scaffolds and further processed them for validation. I prepared extracellular matrix scaffolds for proteomic analysis and generated the proteomic data and results. Nano-liquid chromatography-tandem mass spectrometry was performed together with Dr. rer. med. Oliver Klein and Dipl.-Ing. Grit Nebrich. I analyzed, validated and critically interpreted the proteomic output, performed statistical analysis and defined the final results as distinct attributes of the human liver matrisome. Furthermore, I adapted and employed the assays for the quantification of DNA and TAG as well as histological/immunohistochemical staining and western blot analysis. Finally, I created all figures appearing in this publication based on my results and contributed to make all proteomic data openly accessible.

Publication 2: Daneshgar A, Tang P, Remde C, Lommel M, Moosburner S, Kertzscher U, Klein O, Weinhart M, Pratschke J, Sauer IM, Hillebrandt KH. Teburu - Open source 3D printable bioreactor for tissue slices as dynamic three-dimensional cell culture models. Artif Organs. 2019 Oct;43(10):1035-1041.

My Contribution in Detail: As the lead author of the publication, I contributed an overall share of 80% to all aspect of the project, including conceptualization, designing and fabricating the 3D printable bioreactor, planning, devising and employing all methods and experiments, analyzing and validating data and results as well as writing and revising the manuscript. While I was studying and evaluating the created human liver extracellular matrix scaffolds, I came to understand the importance of standardized and perfusable three-dimensional tissue culture models and the promising combination of such systems with currently available technology to further target and influence cells and matrices. Therefore, I set up the idea of creating a multi-purpose, easy-to-handle bioreactor for the recellularization and dynamic cultivation of scaffolds and tissues. I created the system, so that it can potentially be combined with extending technology to control cells and contribute to the analysis of cell-cell and cell-matrix interactions. The concept of fabricating the bioreactor by 3D printing was set up together with Dr. med. Karl Herbert Hillebrandt. I contributed to the design and fabrication of the 3D printable bioreactor, performed and validated practical flow dynamics and devised and employed de- and recellularization of human liver extracellular matrices. Prof. Dr. med. Igor Maximilian Sauer contributed to the creation of the perfusion chamber for better flow dynamics and named the bioreactor after the Japanese word for table *'Teburu'* to highlight its unique attribute of employing a fixation table. Furthermore, I analyzed and critically interpreted the results, performed histological staining and created all figures with the exception of Figure 2B, which was generated together with Mr. Christopher Remde, and Figure 3A and 3B, which was generated together with Dipl.-Ing. Michael Lommel. Finally, I contributed to make the 3D printable bioreactor *'Teburu'* openly accessible.

Publication 3: Pohl JMO, Raschzok N, Eurich D, Pflüger M, Wiering L, **Daneshgar A**, Dziodzio T, Jara M, Globke B, Sauer IM, Biebl M, Lurje G, Schöning W, Schmelzle M, Tacke F, Pratschke J, Ritschl PV, Öllinger R. Outcomes of Liver Resections after Liver Transplantation at a High-Volume Hepatobiliary Center. J Clin Med. 2020 Nov;9(11):3685.

My Contribution in Detail: As co-author of the publication, I contributed to data acquisition and writing of the manuscript.

_____

Date, Signature and Stamp of First Supervising University Professor / Lecturer

_____

Date and Signature of Doctoral Candidate

Journal Summary List 2019 'Engineering, Biomedical' – Paper 1

Journal Data Filtered By: **Selected JCR Year: 2019** Selected Editions: SCIE,SSCI
Selected Categories: **"ENGINEERING, BIOMEDICAL"** Selected Category
Scheme: WoS
Gesamtanzahl: 87 Journale

Rank	Full Journal Title	Total Cites	Journal Impact Factor	Eigenfactor Score
1	Nature Biomedical Engineering	3,143	18.952	0.014180
2	Annual Review of Biomedical Engineering	4,698	15.541	0.004880
3	MEDICAL IMAGE ANALYSIS	9,028	11.148	0.017100
4	BIOMATERIALS	108,070	10.317	0.089110
5	Bioactive Materials	859	8.724	0.001650
6	Biofabrication	4,311	8.213	0.007470
7	Advanced Healthcare Materials	11,883	7.367	0.027520
8	Acta Biomaterialia	39,268	7.242	0.050720
9	npj Regenerative Medicine	417	7.021	0.001630
10	IEEE TRANSACTIONS ON MEDICAL IMAGING	21,657	6.685	0.030060
11	Bioengineering & Translational Medicine	595	6.091	0.001660
12	Photoacoustics	715	5.870	0.001760
13	Tissue Engineering Part B-Reviews	3,603	5.724	0.004190
14	IEEE TRANSACTIONS ON BIOMEDICAL ENGINEERING	23,928	4.424	0.021150
15	ARTIFICIAL INTELLIGENCE IN MEDICINE	2,953	4.383	0.003370
16	Journal of Neural Engineering	7,240	4.141	0.011940
17	Bio-Design and Manufacturing	99	4.095	0.000180
18	IEEE Transactions on Biomedical Circuits and Systems	3,534	4.042	0.006530
19	COMPUTERIZED MEDICAL IMAGING AND GRAPHICS	2,656	3.750	0.002940
20	EUROPEAN CELLS & MATERIALS	3,088	3.741	0.003140

Selected JCR Year: 2019; Selected Categories: "ENGINEERING, BIOMEDICAL"

Paper 1

A. Daneshgar, O. Klein, G. Nebrich, M. Weinhart, P. Tang, A. Arnold, I. Ullah, J. Pohl, S. Moosburner, N. Raschzok, B. Strücker, M. Bahra, J. Pratschke, I.M. Sauer, K.H. Hillebrandt, The human liver matrisome - Proteomic analysis of native and fibrotic human liver extracellular matrices for organ engineering approaches. Biomaterials. 257 (2020) 120247.

https://doi.org/10.1016/j.biomaterials.2020.120247

Epub 2020 Jul 24.

PMID: 32739662.

Journal Summary List 2019 'Engineering, Biomedical' – Paper 2

Journal Data Filtered By: **Selected JCR Year: 2019** Selected Editions: SCIE,SSCI
Selected Categories: **"ENGINEERING, BIOMEDICAL"** Selected Category
Scheme: WoS
Gesamtanzahl: 87 Journale

Rank	Full Journal Title	Total Cites	Journal Impact Factor	Eigenfactor Score
1	Nature Biomedical Engineering	3,143	18.952	0.014180
2	Annual Review of Biomedical Engineering	4,698	15.541	0.004880
3	MEDICAL IMAGE ANALYSIS	9,028	11.148	0.017100
4	BIOMATERIALS	108,070	10.317	0.089110
5	Bioactive Materials	859	8.724	0.001650
6	Biofabrication	4,311	8.213	0.007470
7	Advanced Healthcare Materials	11,883	7.367	0.027520
8	Acta Biomaterialia	39,268	7.242	0.050720
9	npj Regenerative Medicine	417	7.021	0.001630

50	Regenerative Therapy	258	2.286	0.000510
51	ARTIFICIAL ORGANS	3,977	2.259	0.004390
52	JOURNAL OF BIOMATERIALS APPLICATIONS	2,595	2.220	0.003340
53	Expert Review of Medical Devices	2,143	2.200	0.003390
54	BIOMEDICAL MICRODEVICES	3,425	2.176	0.003570
55	International Journal for Numerical Methods in Biomedical Engineering	1,614	2.097	0.003380
56	Biomedical Engineering Online	3,520	2.059	0.005150
57	Sports Biomechanics	981	2.023	0.001390
58	MEDICAL & BIOLOGICAL ENGINEERING & COMPUTING	5,723	2.022	0.004520

3

Selected JCR Year: 2019; Selected Categories: "ENGINEERING, BIOMEDICAL"

Paper 2

A. Daneshgar, P. Tang, C. Remde, M. Lommel, S. Moosburner, U. Kertzscher, O. Klein, M. Weinhart, J. Pratschke, I.M. Sauer, K.H. Hillebrandt, Teburu - Open source 3D printable bioreactor for tissue slices as dynamic three-dimensional cell culture models, Artif. Organs 43 (2019) 1035–1041.

https://doi.org/10.1111/aor.13518

Epub 2019 Jul 17.

PMID: 31211867.

Journal Summary List 2019 'Medicine, General and Internal' – Paper 3

Journal Data Filtered By: **Selected JCR Year: 2019** Selected Editions: SCIE,SSCI
Selected Categories: **"MEDICINE, GENERAL and INTERNAL"**
Selected Category Scheme: WoS
Gesamtanzahl: 165 Journale

Rank	Full Journal Title	Total Cites	Journal Impact Factor	Eigenfactor Score
1	NEW ENGLAND JOURNAL OF MEDICINE	347,451	74.699	0.660800
2	LANCET	256,199	60.392	0.437300
3	JAMA-JOURNAL OF THE AMERICAN MEDICAL ASSOCIATION	158,632	45.540	0.290050
4	Nature Reviews Disease Primers	7,567	40.689	0.032310
5	BMJ-British Medical Journal	118,586	30.223	0.145170
6	ANNALS OF INTERNAL MEDICINE	58,033	21.317	0.091210
7	JAMA Internal Medicine	17,260	18.652	0.086180
8	PLOS MEDICINE	32,312	10.500	0.065990
9	Journal of Cachexia Sarcopenia and Muscle	3,553	9.802	0.007860
10	Cochrane Database of Systematic Reviews	67,763	7.890	0.134360
11	CANADIAN MEDICAL ASSOCIATION JOURNAL	15,212	7.744	0.016160
12	JOURNAL OF TRAVEL MEDICINE	2,659	7.089	0.006360
13	MAYO CLINIC PROCEEDINGS	15,627	6.942	0.024990

Rank	Full Journal Title	Total Cites	Journal Impact Factor	Eigenfactor Score
35	PANMINERVA MEDICA	806	3.467	0.000660
36	Journal of Clinical Medicine	5,214	3.303	0.010940
37	ANNALS OF MEDICINE	4,510	3.243	0.005190
38	CANADIAN FAMILY PHYSICIAN	3,833	3.112	0.005150

Selected JCR Year: 2019; Selected Categories: "MEDICINE, GENERAL und INTERNAL"

Paper 3

J.M.O. Pohl, N. Raschzok, D. Eurich, M. Pflüger, L. Wiering, A. Daneshgar, T. Dziodzio, M. Jara, B. Globke, I.M. Sauer, M. Bieble, G. Lurje, W. Schöning, M. Schmelzle, F. Tacke, J. Pratschke, P. Ritschl, R. Öllinger, Outcomes of liver resections after liver transplantation at a high-volume hepatobiliary center, J. Clin. Med. 9 (2020) 3685.

https://doi.org/10.3390/jcm9113685

Epub 2020 Nov 17.

PMID: 33212913.

Curriculum Vitae

Mein Lebenslauf wird aus datenschutzrechtlichen Gründen in der elektronischen Version meiner Arbeit nicht veröffentlicht.

List of Publications

- **Daneshgar A**, Klein O, Nebrich G, Weinhart M, Tang P, Arnold A, Ullah I, Pohl J, Moosburner S, Raschzok N, Strücker B, Bahra M, Pratschke J, Sauer IM, Hillebrandt KH. The human liver matrisome - Proteomic analysis of native and fibrotic human liver extracellular matrices for organ engineering approaches. Biomaterials. 2020 Oct;257:120247.

  Impact Factor 2020: 12.479

- **Daneshgar A**, Tang P, Remde C, Lommel M, Moosburner S, Kertzscher U, Klein O, Weinhart M, Pratschke J, Sauer IM, Hillebrandt KH. Teburu – Open source 3D printable bioreactor for tissue slices as dynamic three-dimensional cell culture models. Artif Organs. 2019 Oct;43(10):1035-1041.

  Impact Factor 2020: 3.094

- Pohl JMO, Raschzok N, Eurich D, Pflüger M, Wiering L, **Daneshgar A**, Dziodzio T, Jara M, Globke B, Sauer IM, Bieble M, Lurje G, Schöning W, Schmelzle M, Tacke F, Pratschke J, Ritschl P, Öllinger R. Outcomes of liver resections after liver transplantation at a high-volume hepatobiliary center. J. Clin. Med. *2020, 9(11), 3685.*

  Impact Factor 2020: 4.241

Acknowledgements